The Bone Organ System: Form and Function

ELISE F. MORGAN, GEORGE L. BARNES, AND THOMAS A. EINHORN

I. INTRODUCTION

Bone is a vital, dynamic connective tissue whose structure and composition reflect a balance between its two major functions: provision of mechanical integrity for locomotion and protection, and involvement in the metabolic pathways associated with mineral homeostasis. In addition, bone is the primary site of hematopoiesis, and a rich picture of the complex interplay between the bone organ system and the immune system continues to emerge [1–3].

Beginning with the observations of Galileo, it has been assumed that the shape and internal structure of bone are influenced by the mechanical loads associated with normal function. The 19th century saw active development of this concept, particularly with respect to the cross-sectional geometry of whole bones [4] and to the structure of trabecular bone (see [5, 6] for a review). The most well known of the published works from this time period is by Julius Wolff, who synthesized many others' observations in postulating that the structure of trabecular bone is aligned with the principal stress directions that occur in this tissue during normal skeletal function [7]. In this hypothesis, known by the misnomer "Wolff's Law," Wolff further proposed, as others before him had [8], that this alignment results from a self-regulating functional adaptation process. Although errors in various components of Wolff's writings have been identified [9, 10], what is generally thought of today as Wolff's Law is the overall concept that, in bone, form follows function. This concept underlies much of the scientific investigation of relationships between bone structure and its mechanical and metabolic functions.

In maintaining these structure–function relationships, bone tissue is constantly being broken down and rebuilt in a process called *remodeling*. The cellular link between bone resorbing cells or osteoclasts, and bone forming cells or osteoblasts, is known as coupling. With age, remodeling tends to result in a negative bone balance, in that at each remodeling site slightly less bone is deposited than is resorbed. This negative balance leads to osteopenia and osteoporosis, thus predisposing the bone to fracture during even minimal trauma. However, in normal states, the remodeling activities in bone serve to reduce bone mass where the mechanical demands of the skeleton are low and to add mass at those sites where the demands are repeatedly high. It is worth emphasizing that, were the removal and deposition of bone tissue to occur independently of mechanical considerations, fluctuations in systemic needs for calcium and magnesium could very well be disastrous for the integrity of the skeleton. Hence, bone is a well-designed organ system whose homeostasis depends on processing of external mechanical input and physiological signals from the systemic environment and the transduction of these signals into cellular and chemical events.

II. COMPOSITION AND ORGANIZATION OF BONE

Bone is a composite material consisting of an inorganic and an organic phase. By weight, approximately 60% of the tissue is inorganic matter, 8–10% is water, and the remainder is organic matter [11]. By volume, these proportions are approximately 40%, 25%, and 35%, respectively. The inorganic phase is an impure form of hydroxyapatite ($Ca_{10}[PO_4]_6[OH]_2$), which is a naturally occurring calcium phosphate. The organic phase is composed predominantly (98% by weight) of type I collagen and a variety of noncollagenous proteins, and cells make up the remaining 2% of this phase [12].

A. Organic Phase

The organic phase of bone plays a wide variety of roles, influencing profoundly the structure and also the mechanical and biochemical properties of the tissue. Growth factors and cytokines, and extracellular matrix proteins such as osteonectin, osteopontin, bone sialoprotein, osteocalcin, proteoglycans, and other phosphoproteins and proteolipids, make small contributions to the overall volume of bone but major contributions to its biologic function (see also Chapter 4, Nordin).

Type I collagen is a ubiquitous protein of extremely low solubility, and it is the major structural component of the bone matrix. The type I collagen molecule consists of three polypeptide chains composed of approximately 1000 amino acids each. These chains take the form of a triple helix of two identical 1(I) chains and one unique 2(I) chain cross-linked by hydrogen bonding between hydroxyproline and other charged residues. This produces a very rigid linear molecule that is approximately 300 nm in length. Each molecule is aligned with the next in a parallel fashion and in a quarter-staggered array to produce a collagen fibril. The collagen fibrils are then grouped in bundles to form the collagen fiber. Within the collagen fibril, gaps known as "hole zones" are present between the ends of the molecules. In addition, pores exist between the sides of parallel molecules (Figure 1-1). Noncollagenous proteins or mineral deposits can be found within these spaces, and mineralization of the matrix is thought to be initiated in the hole zones.

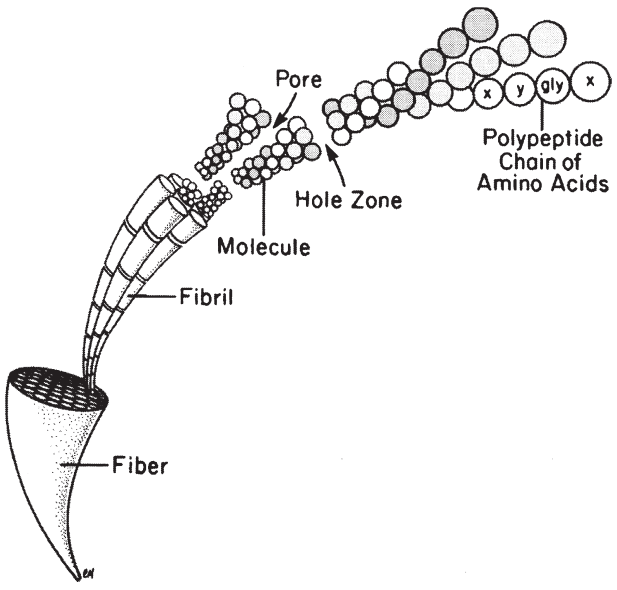

FIGURE 1-1 Collagen fiber and fibril structure with putative locations of pores and hole zones shown. Reprinted with permission from [12].

Several noncollagenous proteins have been identified in bone. One of the more extensively studied of these in bone is osteocalcin (OC) or bone-carboxyglutamic acid-containing protein (bone Gla protein). This is a small (5.8 kDa) protein in which three glutamic acid residues are carboxylated as a result of a vitamin K dependent, post-translational modification. The carboxylation of these residues confers on this protein calcium and mineral binding properties. Osteocalcin is one of the most abundant noncollagenous proteins in bone, accounting for 10–20% of the noncollagenous protein content, and it is closely associated with the mineral phase. Evidence suggests that this bone-specific protein may regulate activities of osteoclasts and osteoclast precursors. However, through characterization of the phenotype of osteocalcin-deficient mice, it was also found that osteocalcin has an important role in inhibiting bone formation and in mineral maturation [13].

Other noncollagenous proteins found in bone may also be important in mineral binding, including nucleation and crystal growth. In addition, several of the bone matrix proteins, such as osteopontin, bone sialoprotein, bone acidic glycoprotein, thrombospondin, and fibronectin, contain arginine–glycine–aspartic acid (RGD) sequences. These amino acid sequences, which are characteristic of cell-binding proteins, are recognized by a family of cell membrane proteins known as integrins. The integrins span the cell membrane and provide a link between the extracellular matrix and the cytoskeleton of the cell. Integrins on osteoblasts, osteoclasts, and fibroblasts provide a means for anchoring these cells to the extracellular matrix. Once anchored, the cells are then enabled to express their phenotype and conduct the types of activities that characterize their functions [14].

Growth factors and cytokines such as transforming growth factor-β (TGF-β), insulin-like growth factor (IGF), osteoprotegerin (OPG), interferon-γ, the tumor necrosis factors (TNFs), the interleukins, and the bone morphogenetic proteins (BMPs 2–10) are present in very small quantities in bone matrix. Such proteins have important effects regulating bone cell differentiation, activation, growth, and turnover (see Chapter 14, Komm). It is also likely that these growth factors serve as coupling factors that link the processes of bone formation and bone resorption (Table 1-1).

B. Inorganic Phase

Bone mineral is not pure hydroxyapatite. The small plate-shaped (20–50 nm long, 15 nm wide, and 2–5 nm thick) apatite crystals contain impurities, most notably carbonate in place of the phosphate groups.

TABLE 1-1 Noncollagenous Proteins of the Extracellular Matrix

Structural matrix proteins	
Osteocalcin	Restricted to the osteoblast lineage. Vitamin K dependent. May regulate osteoclasts and their precursors.
Osteopontin	Expressed by a variety of cells. Highly expressed in bone and inflammatory tissue. Contains an RGD sequence. Supports osteoblast attachment to bone. Member of the small integrin-binding ligand N-linked glycoprotein (sibling) family. Binds and activates MMP-3.
Bone sialoprotein	Made by osteoblasts and hypertrophic chondrocytes. May initiate mineralization. Supports cell attachment. Binds Ca+ with a high affinity. Member of the sibling family. Binds and activates MMP-2.
Decorin	Also known as chondroitin sulfate proteoglycan I. Regulates collagen fibrillogenesis and TGFβ1 activity. Binds to fibrinogen.
Biglycan	Also known as chondroitin sulfate proteoglycan II. Involved in the regulation of fibrillogenesis. Modulates BMP-2 induced osteogenesis.
Osteonectin	Expressed in a variety of connective tissues. Strong affinity for Ca+. May play a role in matrix mineralization.
Enzymatic matrix modifiers	
MMPs	The matrix metalloproteinases (MMPs) includes collagenases (MMP-1 and -13) and gelatinases (MMP-2 and -9). MMPs are required for collagen degradation. Most are expressed in mature chondrocytes and osteoblasts.
TIMPS	Tissue inhibitors of MMPs (TIMPs) are the inhibitors of MMP activity.
Lysyl oxidase	Copper-dependent extracellular enzyme that catalyzes oxidative deamination of elastin and collagen precursors leading to the formation of a mature ECM.
Stromelysin	Member of the MMP family (MMP-3). Degrades most components of the ECM. Activates other MMPs.
Bone morphogens	
TGFβ superfamily	The transforming growth factor β (TGFβ) superfamily of morphogens include TGFβ1-3, the bone morphogenic proteins (BMPs), and the growth and differentiation factors (GDFs). This family of morphogens regulates most steps in chondrogenic, osteogenic, and osteoclastogenic cellular differentiation.
FGFs	Fibroblast growth factors 1 and 2 have angiogenic properties. FGFs promote cellular proliferation.
PDGFs	Platelet-derived growth factors exist in three forms (AA, AB, BB). PDGF is associated with mesenchymal cell chemotaxis and proliferation.

The concentration of carbonate (4–6%) makes bone mineral similar to a carbonate apatite known as dahllite. Other documented substitutions are potassium, magnesium, strontium, and sodium in place of the calcium ions and chloride and fluoride in place of the hydroxyl groups [15]. These impurities reduce the crystallinity of the apatite [16], and in doing so may alter certain properties such as solubility [17]. The solubility of bone mineral is critical for mineral homeostasis and bone adaptation.

The crystal size and crystallinity of bone mineral are altered with certain diseases and therapies. For example, crystal size is decreased with Paget's disease [18] and diabetes [19], but increased in osteopetrotic individuals [20] and with bisphosphonate treatment [21]. Whether osteoporosis is associated with abnormal crystal size or crystallinity is the subject of some controversy [22].

C. Organization of Bone

The skeleton is composed of two parts: the axial skeleton, which includes the bones of the head and trunk, and the appendicular skeleton, which includes all of the bones of the limbs and pelvic girdle. The standard example used in discussions of the macroscale structure of whole bones is the long bone. Long bones such as the tibia, femur, and humerus are divided into three parts: the epiphysis, metaphysis, and diaphysis (Figure 1-2). The *epiphysis* is found at either end of the bone and develops from a center of ossification that is distinct from the rest of the long bone shaft. It is separated from the rest of the bone by a layer of growth cartilage known as the *physis*. The *metaphysis* is the region between the physis and the central portion of the long bone (known as the *diaphysis*). From a structural perspective, the metaphysis is the region of transition from the wider epiphysis to the more slender diaphysis.

Membranes on both the outer and inner surface of the whole bone play important roles in bone modeling and remodeling, as well as in fracture healing. The periosteum lines the outer surface of nearly the entire long bone. It is not present on the articulating surfaces and at ligament and tendon insertion points. The periosteum is composed of two layers: an outer fibrous layer that is in direct contact with muscle and other

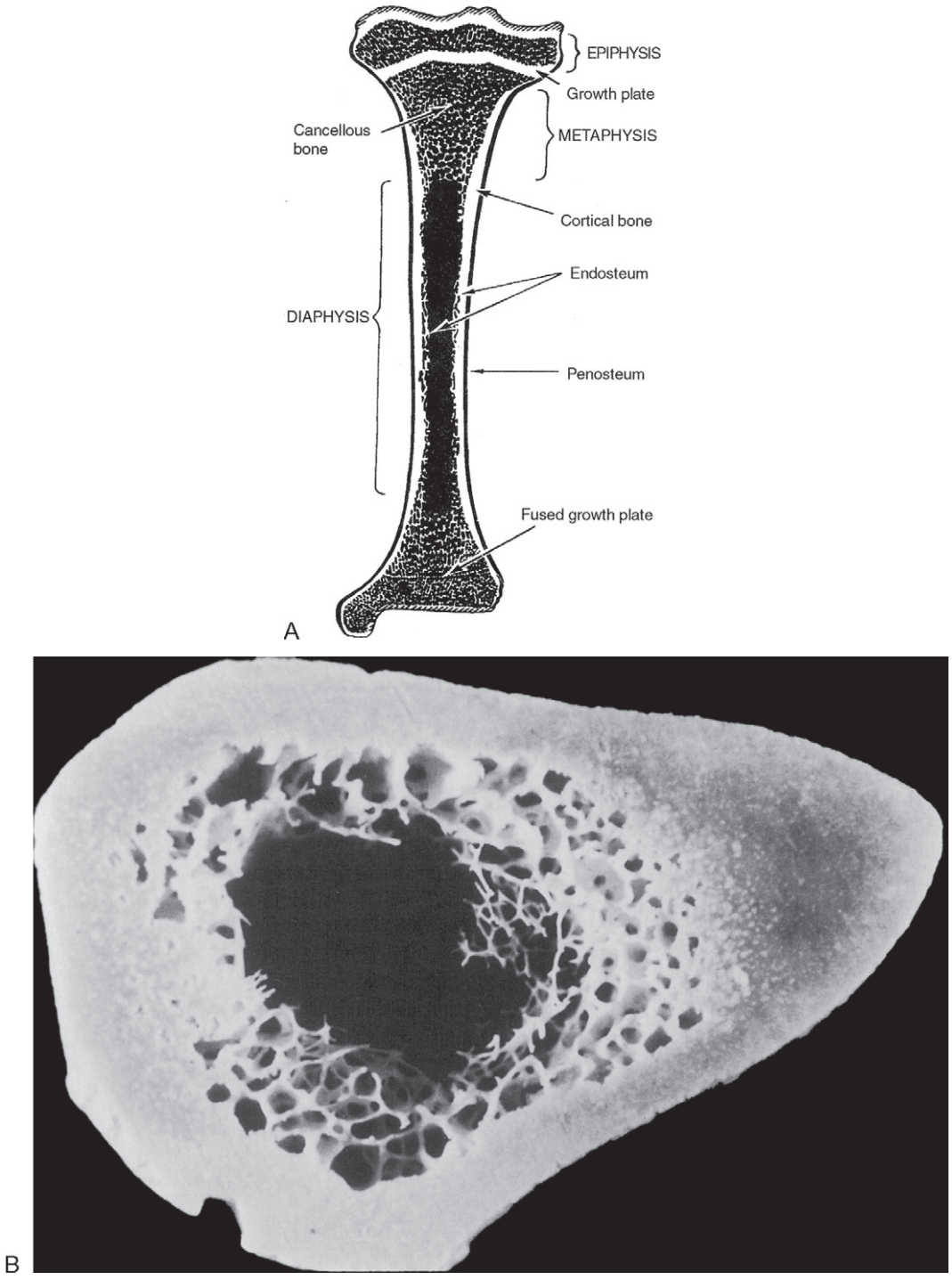

FIGURE 1-2 (A) Sketch of a longitudinal cross-section of a long bone. Reprinted with permission from [102]. (B) Cross-section of the mid-diaphysis of the tibia.

soft tissues, and an inner layer, known as the cambium layer. Whereas the outer layer is much like a sheath of fibrous connective tissue, the cambium layer is populated by uncommitted progenitors of osteoblasts and chondrocytes (Figure 1-3). Through this pool of precursor cells, the periosteum contributes to appositional bone growth during bone development and is responsible for the expansion of the diameters of the

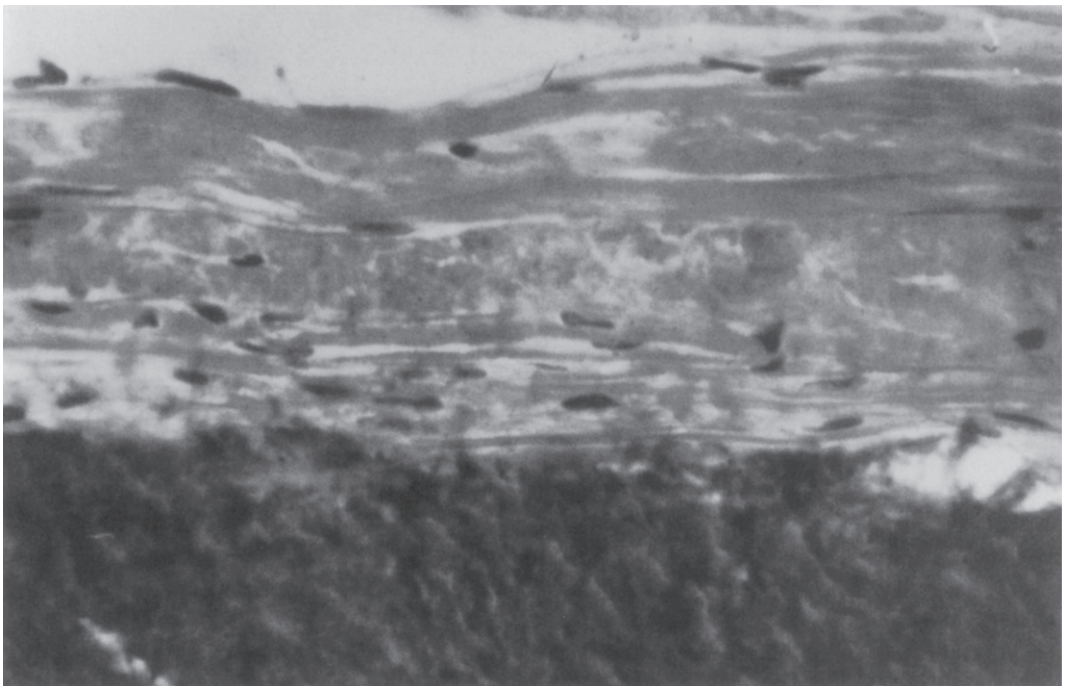

FIGURE 1-3 Magnified view of the periosteum of a long bone. The darker staining tissue at the lower portion of the figure is mineralized cortical bone. Above this is the periosteum, which consists of two layers. The outer layer contains elongated fibroblast-like cells embedded in a fibrous-like tissue. The inner layer, known as the cambium layer, is a loose connective tissue populated by osteoblast and chondrocyte precursors.

long bones with aging. The endosteum lines the inner surfaces of the long bone and consists of bone surface cells, including osteoblasts and bone lining cells.

The building block of bone tissue is the mineralized collagen fibril (~0.1–3 μm in diameter). These fibrils are arranged either as a collection of randomly oriented fibrils known as woven bone (Figure 1-4) or as aligned in thin sheets called lamellae, which are then stacked in a plywood-type arrangement known as lamellar bone (Figure 1-5). Woven bone is considered immature or primitive bone and is normally found in the embryonic and newborn skeletons, in fracture callus, and in some metaphyseal regions of the growing skeleton. Given that fracture healing and skeletal growth are scenarios in which rapid deposition of bone tissue is advantageous, it is perhaps not surprising that woven bone is laid down relatively quickly (as much as 4 μm per day compared to 1 μm per day for lamellar bone). Woven bone is also found in certain bone tumors, in patients with osteogenesis imperfecta, and in patients with Paget's disease. Lamellar bone is the more mature form of bone tissue that results from the remodeling of woven bone or preexisting lamellar tissue. Lamellar bone begins to develop in the human skeleton at approximately 1 month of age, and by the age of 4, most of the bone in the body is lamellar.

In addition to the difference in fibril arrangement, woven and lamellar bone differ somewhat in composition. As compared to lamellar bone, woven bone has a smaller average apatite crystal size and higher cell density, and the distribution of osteocytes appears random rather than closely associated with the mineralized fibril structure (Figures 1-4 and 1-5). Newly formed woven bone is not as highly mineralized as lamellar bone, although the opposite is true when comparing the final degree of mineralization in these two types of tissues. The differences in composition and structure lead to differences in the mechanical behavior. Due to the random orientation of the fibrils, woven bone is more isotropic than lamellar bone; i.e., its mechanical properties such as stiffness and strength do not depend on the direction in which the forces are applied. In contrast, the stiffness and strength of individual lamellae are greatest in the direction of the fibrils. Depending on the distribution of fibril orientation throughout a region of lamellar bone, however, the stiffness and strength of lamellar bone can range from anisotropic (direction-dependent) to nearly isotropic.

In both woven and lamellar bone, the osteocytes reside in small ellipsoidal holes (5 μm minor diameter; 7–8 μm major diameter) called lacunae (Figure 1-6). In lamellar bone, the lacunae are located along the interfaces between lamellae. There are about 25,000 lacunae

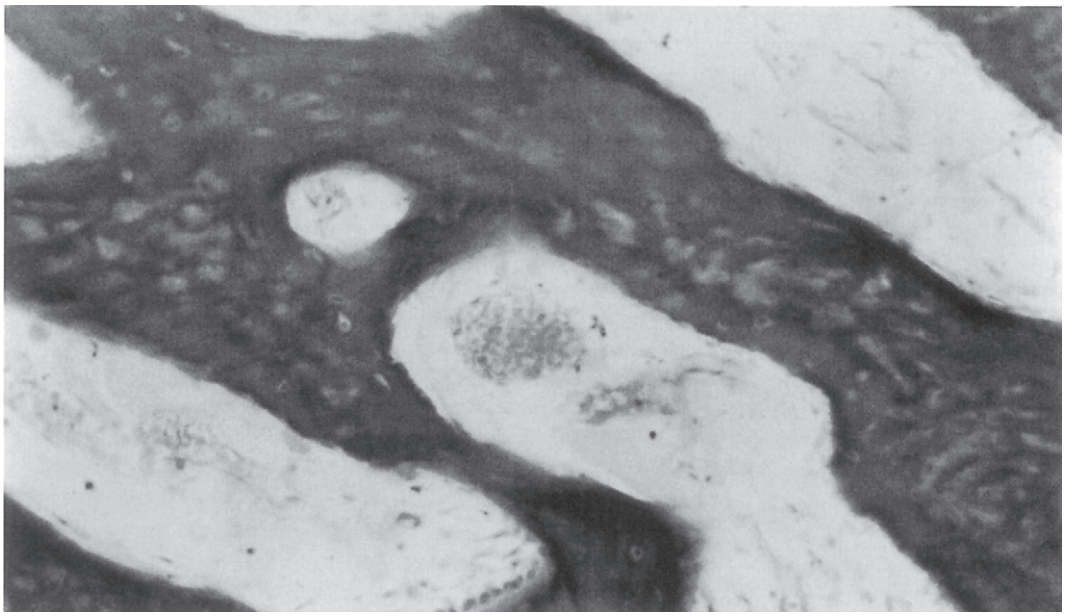

FIGURE 1-4 Woven bone. Note the area of active bone formation (top) and the lack of any particular alignment of the collagen fibrils.

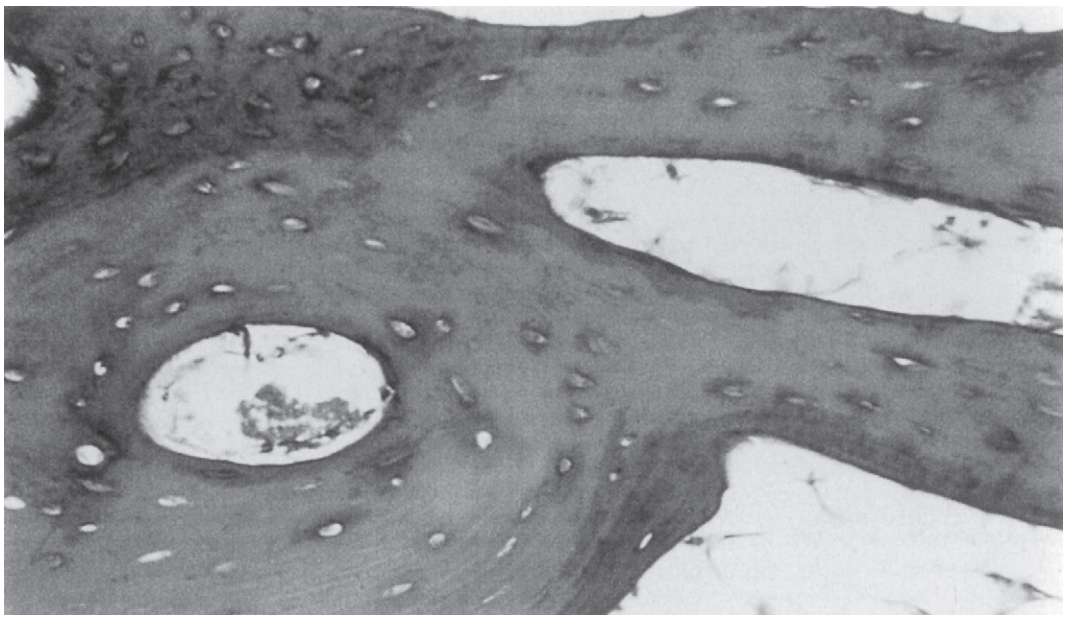

FIGURE 1-5 Lamellar bone. Note the well-delineated orientation of the collagen fibrils and coordinated arrangement of the cells.

per mm^3 in bone tissue, and this number decreases with age [23, 24], although it is not clear if it is further altered with diseases such as osteoporosis [25]. Each osteocyte has dendritic processes that extend from the cell through tiny ($\approx 0.5\,\mu m$ diameter, 3–7 µm long) channels called canaliculi, to meet at cellular gap junctions with the processes of surrounding cells. There are about 50–100 canaliculi per single lacuna and about one million per mm^3 of bone tissue. The lacunar-canalicular network may play a central role in bone mechanotransduction.

Both woven and lamellar bone can occupy fairly large volumes, extending uniformly throughout volumes as large as several cubic millimeters. In particular, lamellar bone is found in the long bone diaphysis as large concentric rings of lamellae in the outer 2–3 mm of the circumference. However, lamellar bone is also commonly

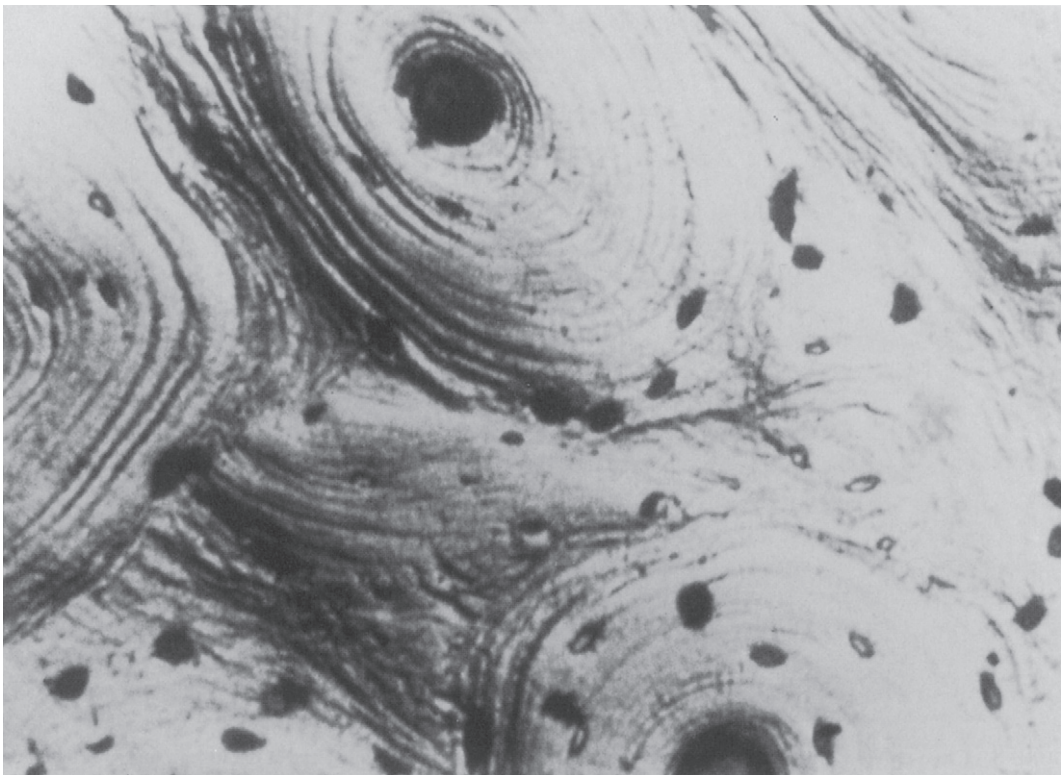

FIGURE 1-6 Scanning electron micrograph of cortical bone showing individual secondary osteons, surrounded by lamellar bone. Osteocytes are housed in the small ellipsoidal lacunae, whose locations are closely associated with the lamellar interfaces.

arranged in smaller cylindrical structures called *secondary osteons* or Haversian systems. These osteons are termed secondary because they are formed through bone remodeling, replacing the previous primary bone tissue. Their diameter and length (typically 200 μm and 1–3 mm, respectively) are determined by the diameter and length of the cutting cone, which is described in the next section on bone remodeling. Each osteon consists of 10–30 concentric rings of lamellae that surround a central cavity, the *Haversian canal*, containing one or more blood vessels and nerves [26] (Figure 1-6). A second type of canal, the Volkmann's canals, run transverse to the osteonal axis, providing a radial path for blood flow through the whole bone. The outer surface of the osteon is lined with a thin (1–2 μm) layer, known as the cement line, consisting of calcified mucopolysaccharides and very little collagen [27]. In the diaphysis, secondary osteons are typically oriented such that their longitudinal axis is aligned with the diaphyseal axis, although evidence exists that in some bones, the osteons loosely spiral around the diaphyseal axis [28, 29]. Although these osteons are often viewed in cross-section, it is important to note that in three dimensions, the osteon is an irregular, anastomosing cylinder.

Most vessels in Haversian and Volkmann's canals have the ultrastructural features of capillaries, although some smaller-sized vessels may resemble lymphatic vessels. When examined histologically, these small vessels contain only precipitated protein; their endothelial walls are not surrounded by a basement membrane. The basement membrane of capillary walls may function as a rate-limiting or selective ion-limiting transport barrier, because all material traversing the vessel wall must go through the basement membrane. The presence of this barrier is particularly important in calcium and phosphorous ion transport to and from bone. The capillaries in the central canals are derived from the principal nutrient arteries of the bone: the epiphyseal and metaphyseal arteries. The vascular system is critical for bone function, not only with respect to nutrient supply but also as a source of cells of both the osteoclast and osteoblast lineage [30, 31].

At the scale of 1–10 mm, there are two types of bone: trabecular bone (also known as cancellous or spongy bone) and cortical bone (also known as compact or dense bone). Trabecular bone is found principally in the axial skeleton and in the metaphyses and epiphyses of long bones (Figure 1-2). It is a highly porous structure consisting of a network of rod- and plate-shaped trabeculae surrounding an interconnected pore space that is filled with bone marrow (Figure 1-7).

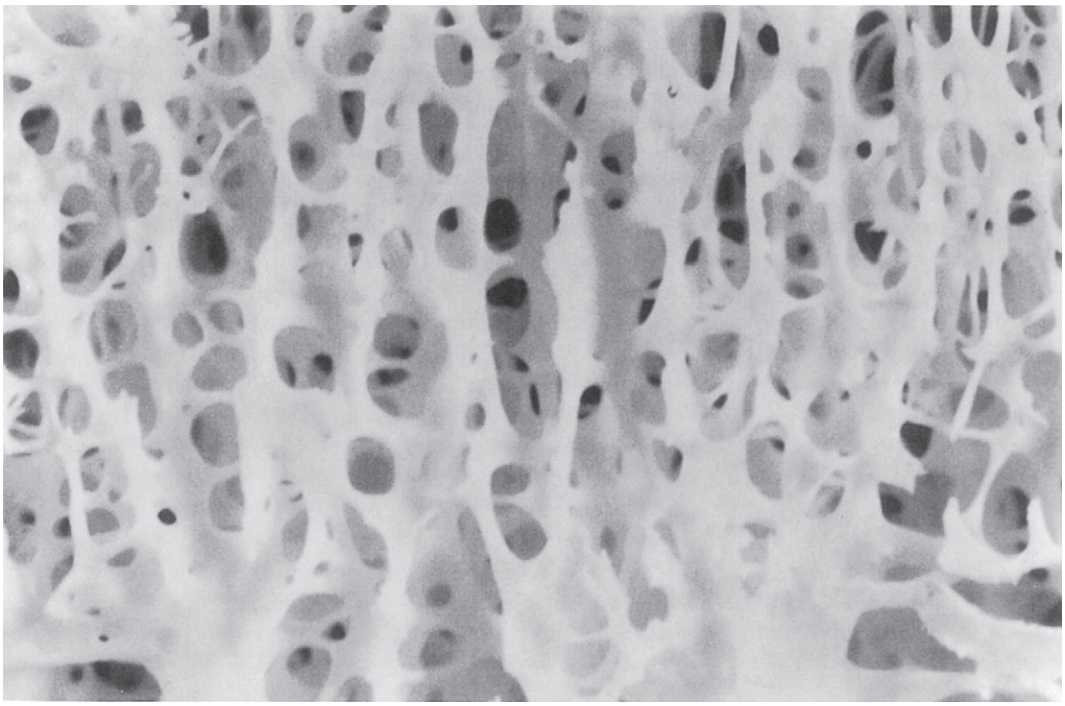

FIGURE 1-7 Trabecular bone. The field of view is approximately 15 mm in width.

Trabeculae range in thickness from 50 to 300 μm and are composed almost exclusively of lamellar bone arranged in packets that are sometimes referred to as hemiosteons. However, the thicker trabeculae can contain secondary osteons, presumably because their thickness is such that nutrient transport via the lacunar-canalicular network alone is insufficient. In the mature human skeleton, cortical bone consists largely of secondary osteons and, to a lesser extent, circumferential lamellae that ring the outer surface of the diaphysis and a type of lamellar bone known as interstitial bone (Figure 1-8). Interstitial bone is merely composed of portions of secondary osteons that were not removed by a cutting cone during remodeling. Both the metaphyses and epiphyses of long bones have a thin shell of cortical bone surrounding the trabecular compartment, and the diaphyses are entirely cortical (Figure 1-2).

The distinction between cortical and trabecular bone can be made largely on the basis of porosity. The porosity of cortical bone ranges only 5–20% and is due to the Haversian and Volkmann's canals and, to a lesser extent, the lacunar and canalicular spaces. Trabecular bone has another scale of porosity due to the marrow space; typical spacing between trabeculae ranges from 100 to 500 μm. The porosity of trabecular bone can range from 40% in the primary compressive group of the femoral neck to more than 95% in the elderly spine. Porosity is the major determinant of the stiffness and strength of trabecular bone [32, 33].

In addition to porosity, the three-dimensional structure of trabecular bone, known as the *trabecular architecture*, can vary tremendously among anatomic sites and with age. Trabecular bone from the vertebral body tends to be predominantly rod-like, while that from the proximal femur contains a more balanced mixture of rods and plates (Figure 1-9). Quantitative descriptors of trabecular architecture such as trabecular thickness and trabecular spacing contribute somewhat independently of porosity to trabecular bone stiffness and strength [34].

With age and also with disuse, trabeculae become progressively thinner and can become perforated by resorption cavities. In certain anatomic sites such as the vertebral body and proximal tibia, age-related changes in trabecular architecture include an increase in the anisotropy of the trabecular structure (Figure 1-10) [35, 36]. With the overall decrease in bone mass with age, this increase in anisotropy helps to preserve the load-carrying capacity of trabecular bone along its main "grain" axis, but at the necessary expense of the load-carrying capacity in other directions. Nonhabitual loading conditions such as impact after a fall can subject trabecular bone to such off-axis loads. Thus, the risk of fracture due to off-axis loads can increase with age to

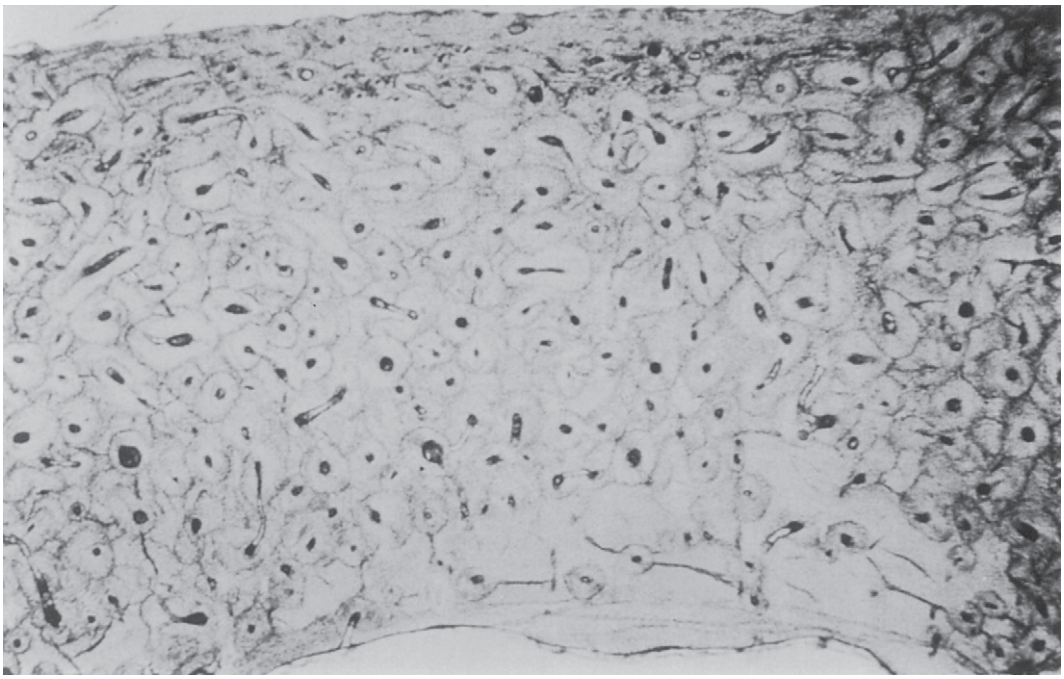

FIGURE 1-8 A transverse section of a long bone diaphysis showing circumferential lamellar bone, secondary osteons, and interstitial bone.

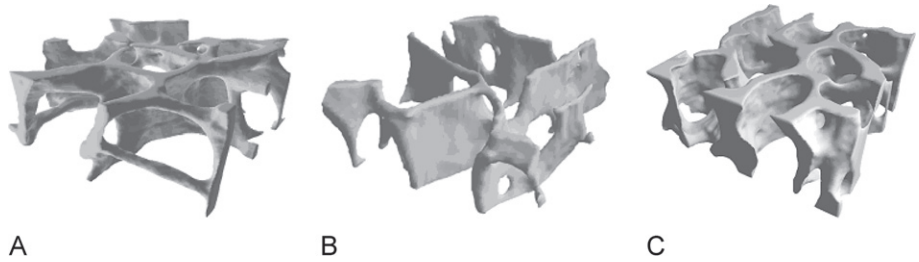

FIGURE 1-9 High-magnification, three-dimensional renderings of trabecular bone from the human (A) vertebra, (B) femoral greater trochanter, and (C) femoral neck. Each volume is 3×3×1 mm^3. From [33].

a greater extent than the decrease in bone mass alone would suggest.

III. CELLULAR COMPONENTS OF BONE

A. Bone Cells

Bone metabolism is regulated by multiple environmental signals including chemical, mechanical, electrical, and magnetic. The local cellular compartment of the bone responds to these environmental signals by modulating the balance between new bone formation and the local resorption of older bone (i.e., remodeling). Three cell types are typically associated with bone homeostasis: osteoblasts, osteocytes, and osteoclasts. These three cell types are derived from two separate stem cell lineages—the mesenchymal lineage and the hematopoietic lineage—underscoring the unique regulation of bone homeostasis and the intimate interactions between the immune system and bone.

B. Mesenchymal Lineage Cells

Bone formation, both embryonic and postnatal, is carried out by the mesenchymal lineage osteoblast. As noted previously, osteoblasts produce the protein matrix of bone made up of type I collagen and several noncollagenous proteins. This protein matrix, referred to as the osteoid, creates a template for mineralization and production of the mature bone. In addition to

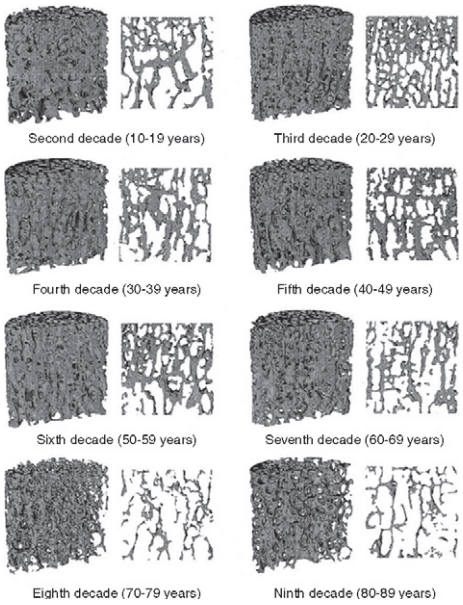

FIGURE 1-10 High-resolution, three-dimensional renderings and two-dimensional cross-sections of trabecular bone from the human proximal tibia in the 2nd–9th decades of life. With age, bone density decreases and an overall deterioration of the trabecular structure occurs. In addition, the tissue becomes more preferentially aligned with the diaphyseal axis of the tibia (here, the vertical direction). This preferential alignment results in anisotropy, or directional dependence, of the structure. The main direction of alignment in the structure is often referred to as the "grain" axis. Reprinted with permission from [36].

bone formation, osteoblasts assist with the initiation of bone resorption by secreting factors that recruit and promote the differentiation of monocytic lineage cells into mature osteoclasts and also by producing neutral proteases that degrade the osteoid and prepare the bone surface for osteoclast-mediated remodeling.

Osteoblasts are derived from mesenchymal stem cells, pluripotent cells that can differentiate into a variety of cell types including myoblasts, adipocytes, chondrocytes, osteoblasts, and osteocytes. The specific lineage selection of an individual mesenchymal stem cell involves a number of coordinated lineage selection steps and the actions of a number of transcriptional regulators whose activities are modulated in response to the local microenvironment (Figure 1-11). Two transcription factors have been demonstrated to be required for osteoblast formation and differentiation: Runx2 and Osterix [37]. The regulatory activity of these central osteoblast regulators is modified by cofactors including members of the Dlx (distaless), Msx, and Hox homeodomain gene families and downstream signal transduction mediators such as the TGF-β superfamily-related SMADs. Runx2 is a member of the runt homology domain transcription factors and acts as a scaffolding protein organizing nuclear complexes at discrete sites on the nuclear matrix associated with active gene transcription. Transgenic knockout-studies have clearly demonstrated the requirement for

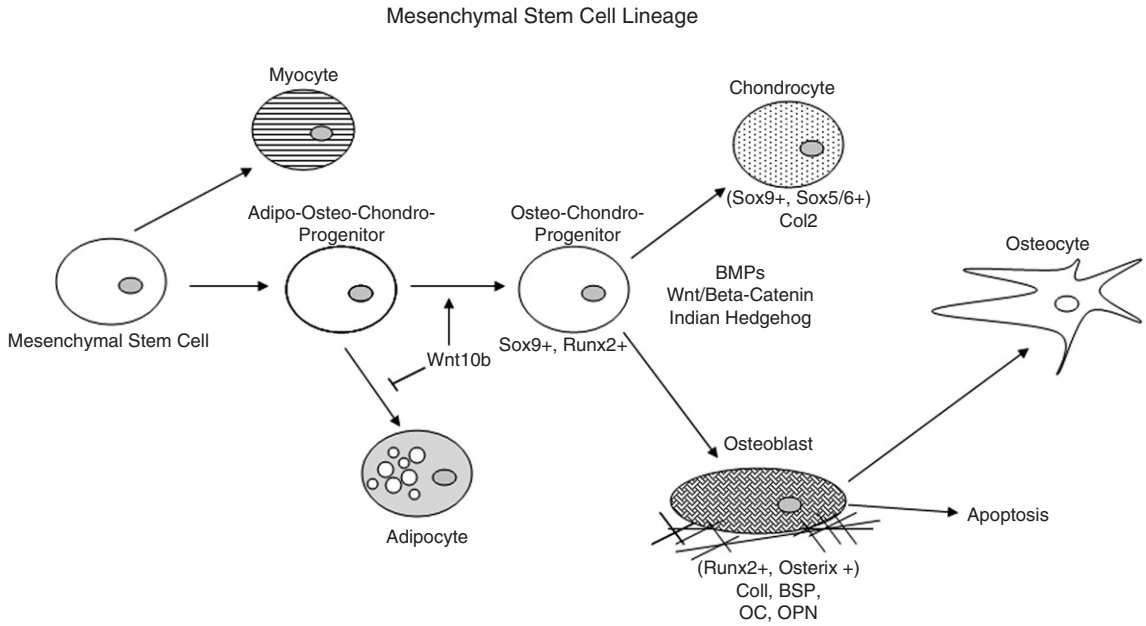

FIGURE 1-11 Graphic representation of the steps involved in osteoblast differentiation from mesenchymal stem cell to matrix expressing mature osteoblast and on to the osteocyte stage.

Runx2 activity for osteoblast differentiation, as these knockoutmice produce no bone during embryogenesis [38]. These Runx2 knockout mice lack osteoblasts and display defects in chondrocyte hypertrophy demonstrating the role of Runx2 in both osteoblast differentiation and chondrocyte maturation. Runx2 regulates the expression of many mature osteoblast-related genes including osteocalcin, bone sialoprotein, osteopontin, and collagen type I. The second required transcription factor for osteoblast differentiation is the zinc finger motif containing factor Osterix. Like Runx2 knockout mice, the Osterix knockouts lack embryonic bone formation and osteoblast differentiation [39]. Unlike the Runx2 deficient animals, Osterix knockouts do not display the defects in chondrocyte hypertrophy, and Runx2 expression levels are comparable to controls. Osterix functions downstream of Runx2 activity as Runx2-/- cells express no Osterix. While the mechanism through which Osterix regulates osteoblast differentiation is poorly understood, it has been noted that in the Osterix knockout mice, the pool of Runx2-expressing pre-osteoblasts express several genes associated with chondrogenesis, suggesting Osterix plays a role in stabilizing osteogenic commitment and osteoblast maturation.

The relative expression and activity of Runx2 and Osterix are regulated by the local microenvironment and, more specifically, the locally produced morphogens to which the cells are exposed. Growth factors including members of the fibroblast growth factors (FGFs), insulin-like growth factors (IGFs), transforming growth factor-beta (TGF-β), bone morphogenetic proteins (BMPs), and Wnts have all been demonstrated to play important roles in regulating embryonic osteoblast differentiation. While each of these morphogens is likely to play some role in postnatal osteoblast differentiation, their role in bone homeostasis is less clear. One exception is the recent data demonstrating that Wnt signaling is an important component of the regulation of bone mineral density (BMD) recognized as a result of mutations in humans. The autosomal recessive disorder osteoporosis pseudoglioma (OPPG), characterized by low bone mass, frequent deformations and fractures, and defects in eye vascularization, has been linked to mutations in lipoprotein-related peptide 5, LRP5 [40–42]. LRP5 is a Wnt co-receptor that, along with the Wnt receptor, frizzled, activates canonical Wnt signaling in cells. Children with OPPG have normal endochondral growth and bone turnover, but their trabecular bone volume is significantly decreased [42a]. Furthermore, gain of function experiments in mature mouse models has shown that organisms with a constitutively activated LRP5 mutation exhibit a high bone mass (HBM) [43]. Thus, these data support the conclusion that canonical Wnt signaling is important in the regulation of postnatal bone mass.

The other mesenchymal lineage cell type found in bone is the osteocyte. Osteocytes are predominantly associated with a mechanosensory function in bone and potentially also a role in Ca+ homeostasis. Osteocytes are a type of osteoblast and thus differentiate from the same mesenchymal lineage under the regulation of the same transcription factors discussed previously [44, 45]. Osteocytes, however, escape apoptosis, reduce their production of matrix molecules, and eventually end up encapsulated in the bone matrix. In the bone they are characterized by their long processes that extend through the lacunocanalicular system of the bone. Osteocytes are in fact the most abundant cellular component of mammalian bones, making up 95% of all bone cells. Relative to the other bone cells, osteocytes are long lived, with estimates running as high as 25 years, as compared to osteoblasts, which are estimated in humans to live approximately an average of 3 months [44]. Osteocytes create an interconnected network in bone allowing for intercellular communications between both neighboring osteocytes and the surface-lining osteoblasts. This interconnection between osteocytes allows for the transmission of mechanical and chemical signals across the network through direct transmission of mechanical forces either through the triggering of integrin force receptors, changes in membrane conformation, chemical signals via the gap junctions, or secreted factors that travel through the extracellular fluid of the lacunocanalicular system [44]. This interconnected signaling allows for the adaptation of bone to the external mechanical and chemical inputs that regulate bone homeostasis.

C. The Hematopoietic Cell Lineage

Bone homeostasis involves the constant remodeling and rebuilding of bone, a process that leads to the replacement of 4–10% of bone each year in humans. While the bone formation side of the equation is carried out by the mesenchymal lineage-derived osteoblasts, the remodeling side of the homeostasis equation in bone is carried out by the hematopoietic lineage osteoclast. Osteoclasts play a role in balancing calcium homeostasis with skeletal remodeling. Histologically, osteoclasts are found at the apex of the classical "cutting cones" in cortical bone and in the resorptive cavities known as Howship's lacunae on trabecular bone surfaces undergoing active remodeling. Osteoclasts are multinucleated cells derived from hematopoietic mononuclear cells [46, 47]. In order to remove bone, newly formed osteoclasts become polarized, form a ruffled membrane, and adhere tightly to the bone matrix via

an $\alpha_v\beta_3$ integrin mediated binding to the bone surface to form the "sealing zone." The osteoclast then secretes acid via H^+-ATPase (for hydroxyapatite dissolution) and proteases including cathepsin K (for matrix protein digestion) into this closed microcompartment along the bone surface referred to as the hemivacuole, thereby removing the underlying bone. By focusing the secretion of these acids and enzymes, osteoclasts are able to move along a bone surface or into a cutting cone slowly solubilizing bone in a defined area without disrupting the surrounding local microenvironment.

Osteoclasts are members of the hematopoietic cell lineage and are derived from mononuclear/macrophage cells (Figure 1-12). A mature multinucleated osteoclast forms by fusion of cells from the hematopoietic and myelomonocytic origin and is therefore a member of the mononuclear phagocyte series and may be thought of as a specialized type of macrophage [46]. Indeed, the bone resorption process employs some of the same cellular machinery as phagocytosis. The early differentiation stages of osteoclast formation depend on the transcription factor PU.1, which regulates c-fms expression along with the transcription factor src [46, 47]. The expression of c-fms, the M-CSF receptor, is a central component of early osteoclast formation as M-CSF responsiveness is required for both monocyte progenitor proliferation and the expression of the receptor activator of NF-κB (RANK), a critical receptor for osteoclast differentiation. The ligand for RANK (RANKL) is the critical cytokine for the final stages in osteoclast differentiation and a member of the TNF-α family of cytokines. The binding of RANKL to the RANK receptor activates NF-κB signaling leading to the formation of mature multinucleated osteoclasts [48]. The activity of RANKL is balanced by the level of expression of its inhibitor osteoprotogerin (OPG), a soluble RANK decoy receptor. It is the local ratio of RANKL to OPG that ultimately determines if osteoclast formation will occur by regulating the amount of available RANKL. In addition to the regulation of osteoclast formation, osteoclast activity can be regulated as can the life span of an osteoclast. Various cytokines have been demonstrated to play a role in enhancing osteoclast activity (IL-1 and RANKL itself) and prolong the life span of an osteoclast (IL-1, IL-6, M-CSF, TNF-α, LPS) [46–48]. Thus osteoclast-mediated bone resorption is regulated by many cytokines associated with inflammation that can regulate osteoclast formation, activity, and apoptosis.

IV. BONE HOMEOSTASIS

A. Osteoblast-Osteoclast Coupling

Bone homeostasis is maintained by the coordinated actions of osteoblast-mediated formation and osteoclast-mediated bone removal. This coordination is referred to as "coupling." The concept of coupling is based on the idea that osteoblasts influence osteoclast formation and activity, and likewise osteoclasts influence osteoblast differentiation and activity (Figure 1-13). Currently, the majority of our understanding of coupling revolves around the influence of osteoblast on osteoclast formation. Osteoblasts express the majority of cytokines that regulate osteoclast progenitor differentiation including M-CSF, RANKL, and OPG in bone, the primary cytokines that regulate osteoclast formation [48]. During osteoblast differentiation, the level of expression of these cytokines changes with the immature osteoblast producing the highest levels of M-CSF and RANKL. Thus, as an osteoblast begins to mature into a matrix-producing bone cell, it signals to local osteoclast precursors with RANKL to differentiate, thereby coupling the new bone formation with the recruitment of new osteoclasts for its subsequent remodeling. By coordinating osteoclast differentiation with osteoblast differentiation, the system stays in balance. Conversely, many researchers believe that osteoclasts signal back to osteoblast progenitors through the release of BMPs and other growth factors that promote osteogenesis from the bone matrix as a part of the bone removal process completing the circle [49].

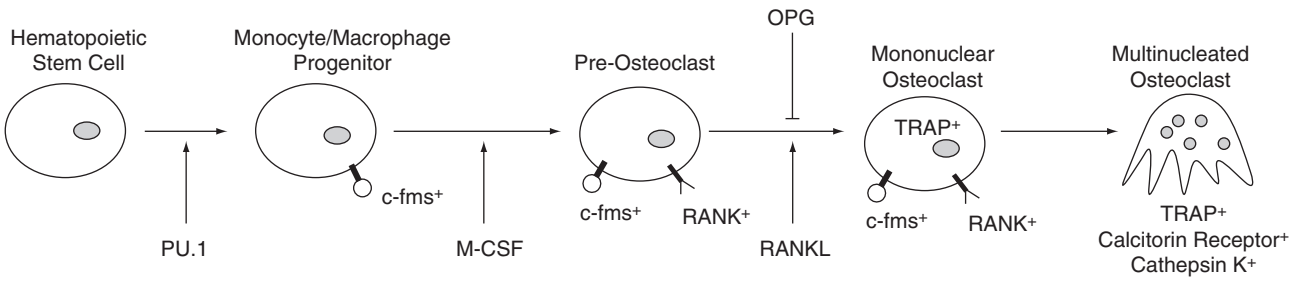

FIGURE 1-12 Graphic representation of the steps involved in osteoclast differentiation from a hematopoietic stem cell to a mature multinucleated osteoclast.

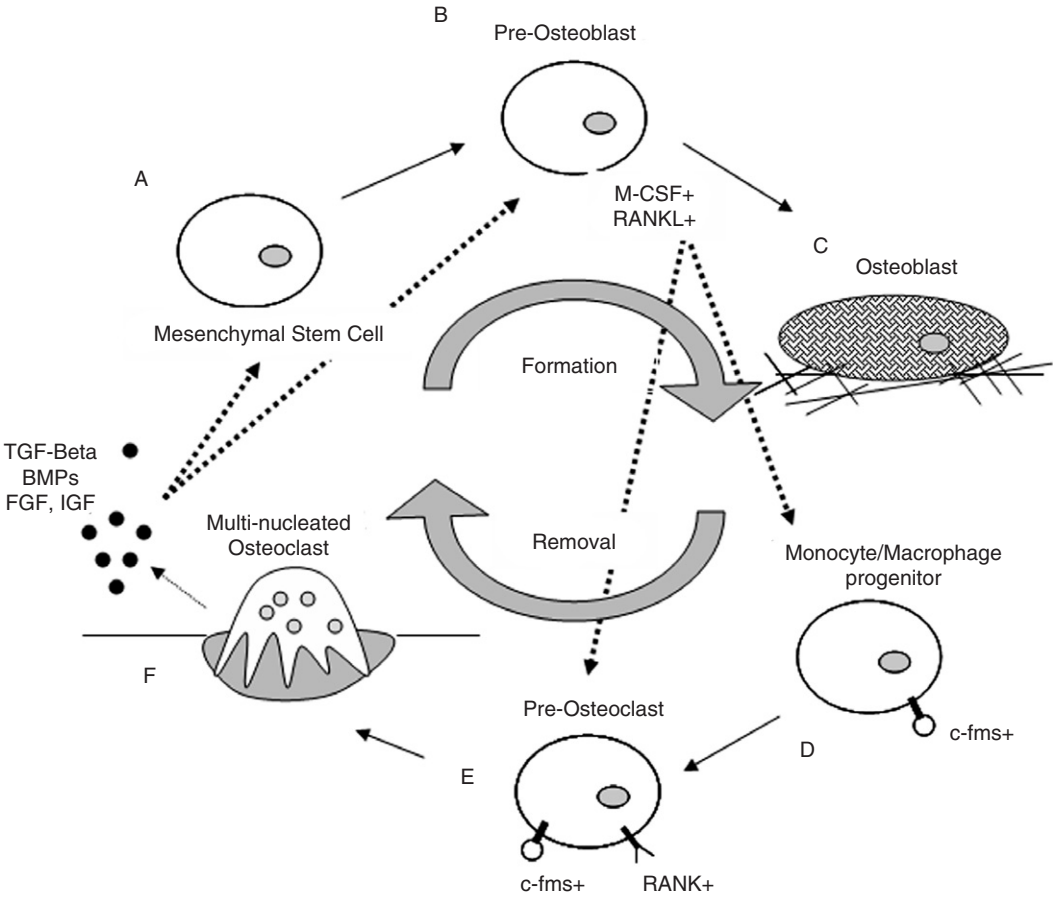

FIGURE 1-13 Graphic representation of the cellular interactions between osteoblast lineage cells (A–C) and osteoclast lineage cells (D–F). Dashed lines indicate cell signaling events important in the coupled differentiation of the respective lineages. Pre-osteolasts (B) express the majority of M-CSF and RANKL that induce osteoclast differentiation (dashed lines indicating effects on progenitor cells and pre-osteoclast). Conversely, morphogens released from bone during osteoclast-mediated removal (F) influence the differentiation of the mesenchymal stem cell and pre-osteoblast (indicated with dashed line)

While the local interactions between osteoblast and osteoclast regulate the local balance of formation and removal, this system was evolutionarily adapted to provide a means of responding to more global mechanical forces and systemic metabolic requirements. The skeleton supports two major functions for the organism as a whole, including load bearing and mineral storage. Bones adapt to the mechanical forces placed upon them. The interconnected osteocyte network is widely perceived to provide mechanosensory feedback that is communicated to the lining osteoblasts [44]. While a multitude of studies have demonstrated that intracellular responses to mechanical input can include increased cAMP, IP3, intracellular calcium, and activation of MAPK pathway, exactly how the mechanical response is transmitted between cells remains unclear [50].

The second primary function of bone is as a mineral store, and bone remodeling plays an important role in systemic mineral homeostasis, with Ca+ being the primary mineral stored in bone. Systemic Ca+ levels are monitored by Ca+ sensors in the parathyroid gland. As Ca+ levels drop, the parathyroid releases parathyroid hormone (PTH). Systemic PTH leads to increased remodeling and the release of Ca+, bringing levels back up into the optimal range. PTH achieves this increase in remodeling primarily through its actions on the osteoblast. PTH increases the expression of the Notch ligand Jagged1 in osteoblasts [51]. It has been demonstrated that osteoblasts can regulate the expansion of the hematopoietic stem cell niche in bone marrow through a Notch-mediated mechanism, and by increasing Jagged1 expression on osteoblasts, PTH leads to an expansion of the hematopoietic lineage from which the osteoclasts are derived. In addition osteoblasts respond to PTH, as well as interleukin-11, prostaglandin E2 (PGE2), and 1,25(OH)2D, by increasing the expression of RANKL and other osteoclast regulatory cytokines leading to increased osteoclast differentiation and activity and decreased osteoclast

apoptosis [52]. Finally, PTH induces increased neutral protease expression by osteoblasts and causes osteoblasts to contract away from the bone surface, exposing the bone and providing the osteoclasts access to the surface. Consequently, systemic release of PTH can induce increased bone resorption and Ca+ release by enhancing osteoclast formation and activity, by increasing osteoblast-mediated preparation of the bone surface by neutral protease secretion, and by providing the osteoclasts access to the bone surface by causing contraction of lining osteoblasts away from the bone.

B. Bone Remodeling

Cortical bone constitutes approximately 80% of the skeletal mass and trabecular bone approximately 20%. Bone surfaces may be undergoing formation or resorption, or they may be inactive. These processes occur throughout life in both cortical and trabecular bone. Bone remodeling is a surface phenomenon, and it occurs on periosteal, endosteal, Haversian canal, and trabecular surfaces. The rate of cortical bone remodeling, which may be as high as 50% per year in the midshaft of the femur during the first 2 years of life, eventually declines to a rate of 2–5% per year in the elderly. Rates of remodeling in trabecular bone are proportionally higher throughout life and may normally be 5–10 times higher than cortical bone remodeling rates in the adult [53].

Historically, bone histologists have described the skeleton as being composed of individual structural units or bone metabolic units (BMU) [17]. The BMU of cortical bone is the osteon or Haversian system. As described previously, the canals are connected to each other by transverse Volkmann's canals and periodically either divide or reunite to form a branching network. Osteons form approximately two-thirds of cortical bone volume, a proportion that falls with age, with the remainder consisting of interstitial bone representing the previous generation of osteons. There are also subperiosteal and subendosteal circumferential lamellae.

In trabecular bone, the BMU is the hemiosteon. In two-dimensional sections, these are shaped like thin crescents about 600 μm long and about 60 μm in depth. Three-dimensionally, these BMUs are actually larger than they appear in two-dimensional histological sections with prolongations in different directions that interlock with adjacent BMUs [54]. These BMUs follow the same shape as the trabecular surface, most of which are concave toward the marrow.

Under normal conditions, the remodeling process of resorption followed by formation is closely coupled and results in no net change in bone mass. As such, the BMU consists of a group of cells that participate in remodeling in a concerted and coordinated fashion. Cortical bone remodeling proceeds via cutting cones and is similar to processes in other hard biological tissues. Cuttings cones, or sheets of osteoclasts, bore holes through the hard bone, leaving tunnels, which appear in cross-section as cavities. The head of the cutting cone consist of osteoclasts that resorb the bone. Following closely behind the osteoclast is a capillary loop and a population of endothelial cells and perivascular mesenchymal cells that are progenitors for osteoblasts and soon begin to lay down the osteoid and refill the resorption cavity. By the end of the process, a new osteon will have been formed. Trabecular bone remodeling occurs on the surface of bone at specific sites. These areas are then filled in with newly formed osteoid. The mechanisms that control the activity and site specificity of this process are unknown.

According to the model proposed by Parfitt, the normal remodeling sequence in bone follows a scheme of quiescence, activation, resorption, reversal, formation, and return to quiescence. In the adult, approximately 80% of trabecular and approximately 95% of intracortical bone surfaces are inactive with respect to bone remodeling [55, 56]. The surface of bone is covered by a layer of thin, flattened lining cells approximately 15 μm in diameter, which arise by terminal transformation of osteoblasts. Between these lining cells and bone is a layer of unmineralized osteoid. These lining cells have receptors for a variety of substances, which are important for initiating bone resorption (PTH, PGE2), and may respond to such substances by resorbing this surface osteoid, which is covering the bone. In doing so, mineralized bone will be exposed, and the activation sequence of bone remodeling may be initiated.

The conversion of a small area of bone surface from quiescence to activity is referred to as activation. The cycle of this response begins with the recruitment of osteoclasts, followed by the initiation of mechanisms for their attraction (chemotaxis) and attachment to the bone surfaces. Several known growth factors may be active in promoting chemotaxis. In addition, several proteins are known to be attachment factors for osteoclasts, such as those that contain the RGD amino acid sequences as noted earlier. Osteopontin, osteocalcin, and osteonectin may be important proteins in this process. In the adult skeleton, activation occurs about every 10 seconds. For intracortical remodeling, osteoclast precursors travel to the site of activation via the circulation, gaining access to the site by either a Volkmann or Haversian canal. In trabecular remodeling, activation occurs at sites that are apposed to bone marrow cells.

In cortical bone, the osteoclast and the cutting cone travel at a speed of about 20 or 40 μm per day, roughly

parallel to the long axis of the bone and about 5–10 μm per day perpendicular to the main direction of advance [57]. In trabecular bone, osteoblasts erode to a depth of about two-thirds of the final cavity; the remainder of the cavity is eroded more slowly by mononuclear cells [58].

The reversal phase is a time interval between the completion of resorption and the initiation of bone formation at a particular skeletal site. Under normal conditions, it lasts about 1–2 weeks. The appearance of new osteoblasts at the base of the resorption cavity depends on chemotaxis for these osteoblasts and their progenitors, as well as conditions that stimulate proliferation. Hence, chemotaxis, attachment, proliferation, and differentiation occur in a stepwise and concerted fashion in order for new bone formation ultimately to take place.

V. BONE MECHANICS

The hierarchical structure of bone, together with evidence that changes in structure can occur with age and disease at many different levels of this hierarchy, renders bone a classic subject for study of mechanical behavior at multiple length scales. In answering a given research question, one may be interested in measuring the mechanical properties of a whole bone, trabecular or cortical bone, single osteons or lamellae, individual mineralized collagen fibrils, or several of the above. Tests performed at each of these length scales can provide insight into bone mechanical properties and, in particular, effects of various age-, disease-, and treatment-related changes in these properties. However, because of the hierarchical complexity of bone structure, it is at best difficult and sometimes impossible to extrapolate across different length scales based only on results from one type of test. For example, a whole bone may be stronger simply because it is larger, not because the tissue itself is any stronger. Similarly, a higher degree of mineralization of the collagen fibrils may not produce a stiffer tissue if those fibrils are not particularly well organized. These examples are just two of the many that motivate consideration of structure–function relationships in bone from the macroscale to microscale to nanoscale.

A. Mechanical Behavior of Whole Bones

The principal advantage of mechanical tests performed on whole bones is that these tests are highly relevant clinically, provided that the manner in which the loads are applied during the test approximates well the *in vivo* loads in the clinical situation of interest. For long bone diaphyses, common *in vivo* loading conditions and *in vitro* mechanical testing configurations include compression, torsion, and bending. Less common is tension. Each of these loading modes results in a characteristic fracture pattern (Figure 1-14). For studies focused on hip fractures, loads are applied *in vitro* in order to simulate gait or fall loading conditions. For the vertebrae, common loading modes include compression and compression combined with bending (specifically, anterior or posterior flexion). Although simple compression and flexion are likely simplified representations of the loads to which vertebrae and motion segments are subjected *in vivo*, these idealized loading conditions do produce clinically observed fracture patterns, including crush, endplate, and wedge fractures (Figure 1-15).

The stiffness and strength of a whole bone are structural properties, not material properties. Structural properties depend on the size and shape of the whole bone as well as on the mechanical properties of the bone tissue itself (material properties). Therefore, quantifying the size and shape of the whole bone can provide some insight into the respective contributions of geometry versus material properties. Principles of engineering mechanics stipulate that the axial stiffness, either in compression or tension, of a structure is proportional to the cross-sectional area, while the bending and torsional stiffnesses of beam-like structures (such as diaphyses) depend on how the material (tissue) is distributed around the axis of bending or twist (Figure 1-16). Material distributed further away from these

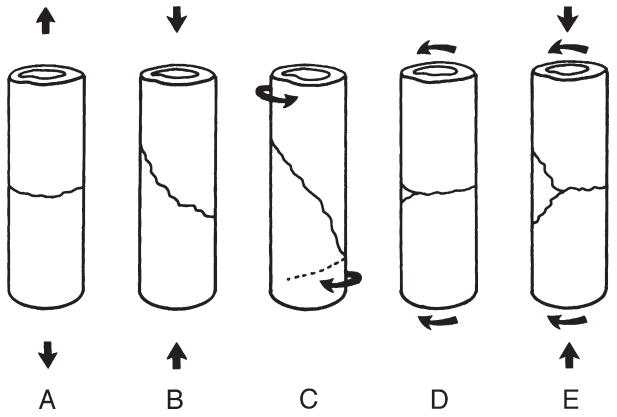

FIGURE 1-14 Fracture patterns in a cylindrical section of bone subjected to different loading configurations. (A) Pure tensile loading produces a transverse fracture. (B) Pure compressive loading produces an oblique fracture. (C) Torsional loading produces a spiral fracture. (D) Bending produces a transverse fracture with a small fragment on the compressive side. (E) Bending superimposed with compression produces a transverse fracture with a larger fragment on the concave side.

FIGURE 1-15 Sagittal section of a vertebral compression fracture.

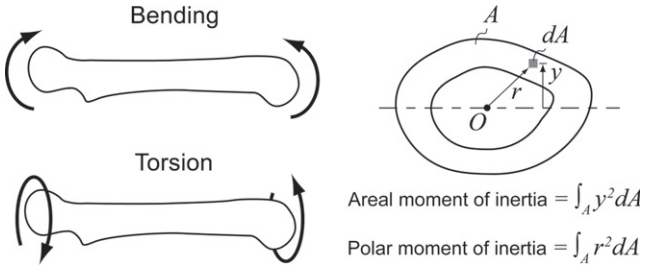

FIGURE 1-16 The bending stiffness of a structure such as a long bone diaphysis is proportional to the areal moment of inertia. If the diaphyseal cross-section is circular, then the torsional stiffnesss is proportional to the polar moment of inertia; otherwise, this proportionality is only approximate. These moments of inertia are geometric quantities that describe how the tissue is distributed with respect to the axis of bending (shown here as the dotted line on the diaphyseal cross-section) or the axis of torsion (the line that passes through point *O* and that is directed out of the plane of the figure).

axes contributes more to resisting the applied bending and torsional loads than does material near the axes. Two geometric properties, the *areal moment of inertia* (also known as the cross-sectional moment of inertia) and *polar moment of inertia*, quantify this distribution in manners relevant for bending and torsion, respectively. These geometric properties can change with physical activity and with aging. For example, with age, both the outer and inner diameter of the diaphysis increase due to a combination of endosteal resorption and periosteal bone formation. The net result is a thinner cortex and smaller cross-sectional area, but also an increase—or at least less of a decrease—in areal moment of inertia and polar moment of inertia [59, 60]. The changes in moment of inertia can serve to mitigate the mechanical consequences of the age-related decline in bone mass. Comparisons of cross-sectional geometry in femoral diaphyses of different inbred mouse strains provide a powerful illustration of the independent contributions of tissue properties and bone size and structure to the mechanical properties of whole bones [61–63].

If the bone is straight, prismatic (the cross-sectional geometry does not change along the length of the structure), and if it is of uniform composition, it is straightforward to calculate the Young's modulus or shear modulus (defined in the next section) of the bone tissue from the results of a test performed on the whole bone [64]. Of course, none of these three descriptors is accurate for vertebral bodies and diaphyses. For the latter, one can calculate an effective elastic modulus of the tissue if the true cross-sectional geometry and its variation along the diaphyseal axis are included in the calculations. However, without accounting for the true geometry of the specimen, substantial errors in the modulus can result [65].

B. Mechanical Behavior of Bone Tissue

Bone tissue is subjected to a wide variety of mechanical demands during activities of daily living and during nonhabitual scenarios such as trauma. Experiments on the mechanical behavior of bone tissue determine the ability of the tissue to meet to those demands. In working with bone tissue, one can avoid the confounding influences of specimen size and shape by preparing tissue samples of regular geometry such that the geometry can be easily accounted for. With this approach, the applied loads can be expressed easily in terms of *stress* rather than force, and the deformation that the specimen undergoes as a result of the applied loads can be expressed in terms of *strain* rather than displacement. Stress is the force per unit area acting on a specimen and thus quantifies the intensity of the force. For a specimen of regular geometry, it is easily calculated by dividing the applied force by the cross-sectional area (Figure 1-17). There are two kinds of stresses: normal stresses and shear stresses. Normal stresses act either to pull the specimen apart (tensile stress) or to shorten or compact it (compressive stress), and shear stresses act to slide one part of the specimen relative to another part. In general, regions of bone tissue are subjected to both normal and shear stresses during normal skeletal function (Figure 1-18).

Strain is a measure of how the specimen deforms, but unlike displacement, the deformation is expressed in terms of a *relative* change in the size or shape of the specimen (Figure 1-17). Normal strains, whether tensile or compressive, quantify the change in length of the specimen relative to its original length. Shear strain quantifies the change in angle of two lines in the material that were originally perpendicular to each other. Strain is dimensionless and is often expressed in microstrain (10^{-6} mm/mm) or percent (10^{-2} mm/mm).

How much strain a specimen of bone tissue will undergo in response to an applied stress depends on the stiffness of the tissue. The material property that

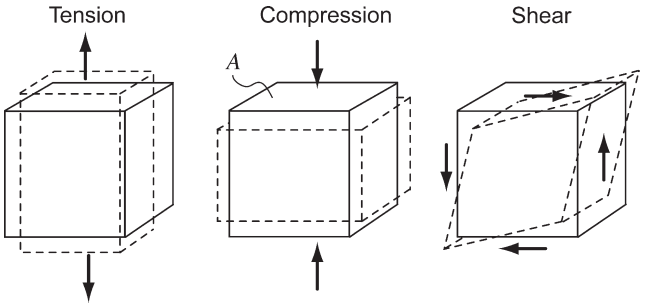

FIGURE 1-17 Normal and shear stresses acting on a specimen of tissue produce normal and shear strains. The dotted lines represent the specimen that is deformed under the action of the applied forces. Whether the applied force is tensile, compressive, or shear, the stress is calculated by dividing the magnitude of the force by the area over which the force is applied (denoted here by *A*). Tensile and compressive stresses cause tensile and compressive strains, respectively, along the direction of the applied force; however, they also cause contraction and expansion, respectively, in the perpendicular directions. The latter effect is quantified by the Poisson's ratio, which is defined as the ratio of transverse to longitudinal strain. Shear strain represents the deformation of the specimen that consists of a change of angle between two lines that were originally perpendicular to each other.

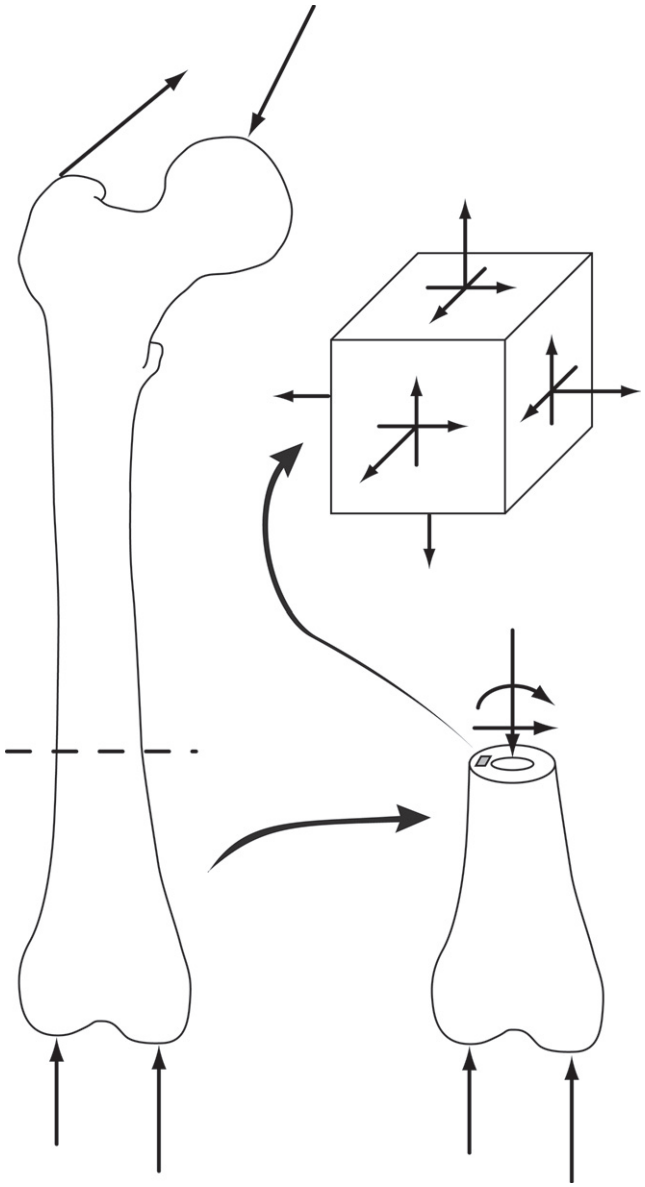

FIGURE 1-18 During normal skeletal function, including gait, regions of bone tissue are subjected to a combination of normal and shear stresses. In the most general case, a region of tissue is subjected to normal and shear stresses on each face. The state of stress shown for this specimen is a multiaxial stress state.

describes stiffness is the elastic modulus or *Young's modulus*. The Young's modulus is defined from a uniaxial test (stress applied along one direction only); it is the slope of the initial portion of the *stress–strain curve*, which is a plot of the applied stress against the normal strain in the direction of applied stress (Figure 1-19). Similarly, the shear modulus is defined as the slope of the initial portion of the shear stress–(shear) strain curve. For cortical bone, the stress–strain curves are fairly linear at low values of stress [66], making reproducible measurement of the modulus straightforward. In contrast, trabecular bone exhibits nonlinearity even at low stresses, and care must be taken to calculate the curve's slope in a manner that is standardized across specimens and experiments [67].

As mentioned briefly in Section II, most types of bone tissue exhibit elastic anisotropy in that the elastic modulus differs depending on the direction of applied load. In the most general case, the type of anisotropy exhibited by bone tissue is orthotropy [68, 69], which means that there is a different elastic modulus along each of three mutually perpendicular directions (Figure 1-20). Some types of bone tissue (e.g., woven bone) are isotropic in that the elastic modulus is the same in all directions. Finally, some types of bone tissue (e.g., cortical bone with a secondary osteon structure and trabecular bone from the vertebral body) exhibit an intermediate class of anisotropy, known as transverse isotropy. For transversely isotropic materials, the elastic modulus is distinct along the direction of the main grain of the tissue but is the same in all directions perpendicular to the grain axis.

In the context of osteoporosis, it is clearly of interest to determine the strength of a specimen of bone tissue. For a uniaxial test, strength is defined either as the ultimate stress (the maximum value of stress that the specimen can bear) or the yield stress. The latter is technically the stress above which the tissue no longer behaves elastically; that is, if the specimen is loaded above the yield stress and then unloaded to zero stress, the specimen will show some permanent deformation and/or a reduction in stiffness upon reloading. In practice, the yield stress and yield strain are defined from the stress–strain curve using an offset method (Figure 1-19).

Determining the strength of a specimen when it is subjected to a multiaxial stress state (a combination of normal and/or shear stresses acting along multiple directions) is more challenging with respect to the experimental methods, but this type of test is clinically relevant, given the complexity of the tissue's mechanical environment *in vivo*. This task is further complicated by fact that strength, like elastic modulus, is anisotropic, being higher along the grain axis than along a direction oblique to this axis. Thus, whether a specimen will fail depends not only on the magnitudes and types of the applied stresses, but also on the orientation of these stresses with respect to the specimen microstructure. Development of multiaxial failure criteria for bone tissue is the subject of ongoing research [70–72].

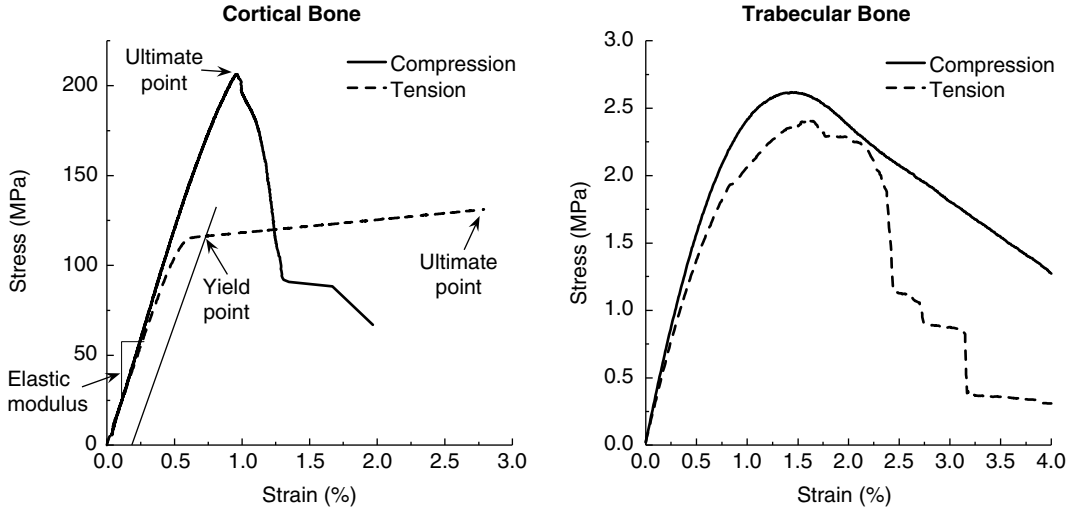

FIGURE 1-19 Stress–strain curves for cortical and trabecular bone in both compression and tension. The elastic modulus is the slope of the initial portion of the curve. Two measures of strength, the yield stress and ultimate stress, are the values of stress at the yield and ultimate points, respectively. In practice the yield point is defined using an offset method: This point is the intersection of the stress–strain curve with a line that has a slope equal to the elastic modulus but that is offset along the strain axis by a certain amount (typically, 0.2%). Data from [33, 103].

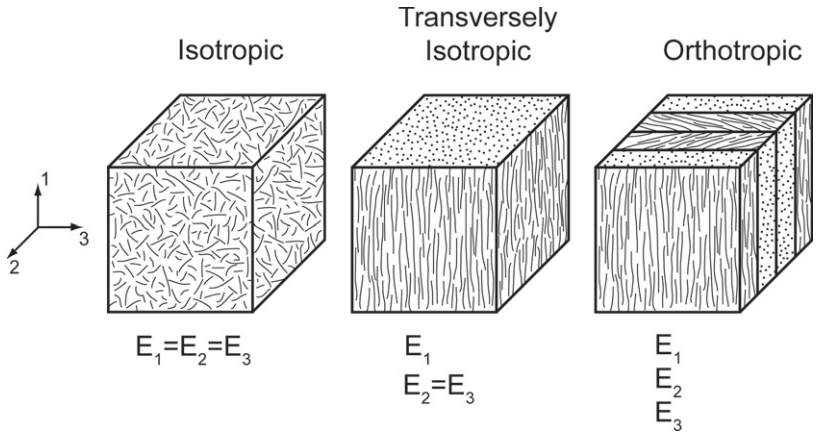

FIGURE 1-20 Three types of anisotropy are typically encountered in bone tissue. If the mineralized collagen fibrils have no particular orientation (such as in woven bone), the tissue is isotropic, and the elastic modulus measured in each of the three directions shown is the same. If the fibrils all have a single, consistent orientation, the tissue is transversely isotropic. The elastic modulus is higher along the direction of the fibrils (the grain axis) but is the same in all directions perpendicular to this axis. Cortical bone composed of secondary osteons is nearly transversely isotropic; in this case the osteons are the "fibrils." Finally, if there are several preferred orientations of the fibrils, such as shown here in a schematic of lamellar bone, the tissue is orthotropic. In this case, the elastic modulus is different along each of the three directions shown. In general, trabecular bone is also orthotropic.

Measures of strength provide a quantitative but essentially dichotomous description of failure, and it is helpful to supplement these measures with investigations of what the mechanisms of failure are for a given type of bone tissue. Failure mechanisms are dictated by not only the nature of the applied loads, but also the composition and microstructure of the tissue. Both cortical bone and trabecular bone are stronger in compression than tension, which reflects the fact that the inorganic phase is stronger in compression than tension. The organic phase contributes to the ductility and toughness of the tissues. *Ductility* is quantified by the amount of strain that the specimen can withstand before complete fracture. *Toughness* is defined in one of two ways, either as the amount of energy that the specimen can absorb prior to complete fracture (also known as the *work to failure* or energy to failure) or as the resistance of the tissue to the initiation and propagation of cracks. The latter is often referred to as the *fracture toughness*. Both the ductility and toughness of intact bone tissue are substantially higher than that of apatite and heat-treated bone tissue [73, 74], suggesting that the organic phase is indeed critical in these two aspects of bone failure. However, the microstructure of bone tissue also plays a role. In cortical tissue, crack growth often initiates at pores such as lacunae and Volkmann's canals and appears to arrest, at least temporarily, at cement lines, leaving secondary osteons intact [27, 75, 76]. For tensile loading along the grain axis, continued crack growth results in debonding of osteons from the interstitial bone and transverse fracture of the osteons themselves, giving the appearance on the fracture surfaces of the specimen that the osteons have "pulled out" of the surrounding tissue [77, 78]. For compressive loading, the osteons tend to fracture oblique to their longitudinal axis, and little pull-out is observed [78].

Crack initiation and propagation are also observed in trabeculae prior to complete, macroscopic failure of trabecular bone, and the extent of microcracking in a given region of trabecular bone appears to be related to the magnitudes of the strains that the region has experienced during loading [79]. As a consequence of the highly porous structure of trabecular bone, even simple loading conditions such as uniaxial compression applied to the entire specimen can produce a wide distribution of stresses and strains in the tissue comprising the trabeculae. Even at low magnitudes of applied stress, some tissue-level strains can be high enough to cause local yielding of the tissue and a concomitant decline in the mechanical properties of the entire specimen of trabecular bone [80].

Although the bulk of the work to date on the mechanical properties of bone tissue has been performed on specimens 1–10 mm in scale, a rapidly growing body of research has focused on micro- and nanoscale properties. Micromechanical tests on osteons and single trabeculae seek to characterize the elastic and failure properties of these small structures within cortical and trabecular bone [81–88]. Osteon push-out tests have been developed to quantify the shear strength of cement lines [89, 90]. In addition, several techniques, including acoustic microscopy and nanoindentation, allow measurement of mechanical properties of regions of

bone tissue composed of just one or several lamellae [91–101]. When combined with other high-resolution imaging and compositional measurement techniques such as x-ray tomography, Raman microspectroscopy, backscattered electron imaging, and infrared (IR) spectroscopy, these nanoscale testing methods enable investigation of relationships among composition, structure, and mechanical function at a very fine level of detail.

VI. SUMMARY

Bone is a complex, hierarchically organized organ system whose composition and structure are closely related to, and in many ways controlled by, the functional demands made upon it. Bone tissue is a composite material composed of a proteinaceous extracellular matrix impregnated with impure apatite crystals. In this sense, the structure and mechanical properties of bone tissue are similar to engineering composite materials such as fiberglass. However, bone tissue is a living tissue that is constantly undergoing turnover via coordinated activities by osteoblasts, osteoclasts, osteocytes, and their precursors. Through this process of bone remodeling, bone is an organ system that can respond relatively quickly to changes in metabolic and structural needs.

Recent and ongoing research has continued to enhance understanding of cellular and hormonal control of bone remodeling. In particular, knockout studies have played essential roles in identifying key transcription factors and signaling pathways involved in bone formation, resorption, and mechanotransduction. Several of these studies and others have linked abnormalities in signaling with changes in bone mechanical properties. Although the picture is by no means complete, it is clear that diseases such as osteoporosis can involve deficits in bone mechanical properties at multiple length scales and that the underlying causes of these deficits can be associated with multiple aspects of bone homeostasis. The concepts presented in this chapter provide a framework for further elucidation of the biological and biomechanical mechanisms underlying the close relationship between form and function in bone.

REFERENCES

1. I. A. Bab and T. A. Einhorn, Polypeptide factors regulating osteogenesis and bone marrow repair. *J Cell Biochem*. **55**, 358–365 (1994).
2. M. Horowitz and R. L. Jilka, Colony stimulating factors in bone remodeling. In *Cytokines and Bone Metabolism* (M. Gowen, ed.). CRC Press, Boca Raton, FL, 185–227 (1992).
3. M. N. Wein, D. C. Jones, and L. H. Glimcher, Turning down the system: Counter-regulatory mechanisms in bone and adaptive immunity. *Immunol Rev*. **208**, 66–79 (2005).
4. C. Bell, *Animal Mechanics, or Proofs of Design in the Animal Frame*. Morrill Wyman, Cambridge, MA, 1827.
5. J. C. Koch, The laws of bone architecture. *Am J Anat*. **21**, 177–298 (1917).
6. H. Roesler, The history of some fundamental concepts in bone biomechanics. *J Biomech*. **20**, 1025–1034 (1987).
7. J. Wolff, *The Law of Bone Remodelling*. Springer-Verlag, Berlin, New York, 1986.
8. W. Roux, *Der Zuchtende Kampf der Teile, oder die "Teilauslese" im Organismus ("Theorie der Funktionellen Anpassung")*. Wilhelm Engelmann, Leipzig, 1881.
9. J. E. Bertram and S. M. Swartz, The "law of bone transformation": A case of crying Wolff? *Biol Rev Camb Philos Soc*. **66**, 245–273 (1991).
10. S. C. Cowin, The false premise of Wolff's law. *Forma*. **12**, 247–262 (1997).
11. J. K. Gong, J. S. Arnold, and S. H. Cohn, Composition of trabecular and cortical bone. *Anat Rec*. **149**, 325–332 (1964).
12. T. A. Einhorn, Bone metabolism and metabolic bone disease. In *Orthopaedic Knowledge Update 4 Home Study Syllabus* (J. W. Frymoyer, ed.). Am Acad Orthop Surg., Rosemont, 69–88 (1994).
13. A. L. Boskey, S. Gadaleta, C. Gundberg, S. B. Doty, P. Ducy, and G. Karsenty, Fourier transform infrared microspectroscopic analysis of bones of osteocalcin-deficient mice provides insight into the function of osteocalcin. *Bone*. **23**, 187–196 (1998).
14. E. Ruoslahti, Integrins. *J Clin Invest*. **87**, 1–5 (1991).
15. D. McConnell, The crystal structure of bone. *Clin Orthop*. **23**, 253–268 (1962).
16. H. Ou-Yang, E. P. Paschalis, W. E. Mayo, A. L. Boskey, and R. Mendelsohn, Infrared microscopic imaging of bone: Spatial distribution of CO3(2–). *J Bone Miner Res*. **16**, 893–900 (2001).
17. F. S. Kaplan, W. C. Hayes, T. M. Keaveny, A. L. Boskey, T. A. Einhorn, and J. P. Iannotti, Form and function of bone, In *Orthopaedic Basic Science* (S. R. Simon, ed.). Am. Acad. Orthop. Surg., 127–184 (1994).
18. E. S. Siris, Paget's disease of bone. *J Bone Miner Res*. **13**, 1061–1065 (1998).
19. T. A. Einhorn, A. L. Boskey, C. M. Gundberg, V. J. Vigorita, V. J. Devlin and M. M. Beyer, The mineral and mechanical properties of bone in chronic experimental diabetes. *J Orthop Res*. **6**, 317–323 (1988).
20. A. L. Boskey and S. C. Marks, Jr., Mineral and matrix alterations in the bones of incisors-absent (ia/ia) osteopetrotic rats. *Calcif Tissue Int*. **37**, 287–292 (1985).
21. P. Fratzl, S. Schreiber, P. Roschger, M. H. Lafage, G. Rodan, and K. Klaushofer, Effects of sodium fluoride and alendronate on the bone mineral in minipigs: A small-angle X-ray scattering and backscattered electron imaging study. *J Bone Miner Res*. **11**, 248–253 (1996).
22. A. L. Boskey, Bone mineral and matrix. Are they altered in osteoporosis? *Orthop Clin North Am*. **21**, 19–29 (1990).
23. M. G. Mullender, D. D. Vandermeer, R. Huiskes, and P. Lips, Osteocyte density changes in aging and osteoporosis. *Bone*. **18**, 109–113 (1996).
24. D. Vashishth, O. Verborgt, G. Divine, M. B. Schaffler, and D. P. Fyhrie, Decline in osteocyte lacunar density in human cortical bone is associated with accumulation of microcracks with age. *Bone*. **26**, 375–380 (2000).

25. M. G. Mullender, S. D. Tan, L. Vico, C. Alexandre, and J. Klein-Nulend, Differences in osteocyte density and bone histomorphometry between men and women and between healthy and osteoporotic subjects. *Calcif Tissue Int*. **77**, 291–296 (2005).
26. G. Marotti and A. Z. Zallone, Changes in the vascular network during the formation of Haversian systems. *Acta Anat (Basel)*. **106**, 84–100 (1980).
27. D. B. Burr, M. B. Schaffler, and R. G. Frederickson, Composition of the cement line and its possible mechanical role as a local interface in human compact bone. *J Biomech*. **21**, 939–945 (1988).
28. J. Cohen and W. H. Harris, The three-dimensional anatomy of the Haversian system. *J Bone Joint Surg*. **40A**, 419–434 (1958).
29. S. Mohsin, D. Taylor, and T. C. Lee, Three-dimensional reconstruction of Haversian systems in ovine compact bone. *Eur J Morphol*. **40**, 309–315 (2002).
30. S. Shi and S. Gronthos, Perivascular niche of postnatal mesenchymal stem cells in human bone marrow and dental pulp. *J Bone Miner Res*. **18**, 696–704 (2003).
31. I. M. Shapiro, E. E. Golub, B. Chance, C. Piddington, O. Oshima, O. C. Tuncay, P. Frasca, and J. C. Haselgrove, Linkage between energy status of perivascular cells and mineralization of the chick growth cartilage. *Dev Biol*. **129**, 372–379 (1988).
32. D. R. Carter and W. C. Hayes, The compressive behavior of bone as a two-phase porous structure. *J Bone Joint Surg*. **59–A**, 954–962 (1977).
33. E. F. Morgan and T. M. Keaveny, Dependence of yield strain of human trabecular bone on anatomic site. *J Biomech*. 34, 569–577 (2001).
34. D. Ulrich, B. Van Rietbergen, A. Laib, and P. Rueegsegger, The ability of three-dimensional structural indices to reflect mechanical aspects of trabecular bone. *Bone*. **25**, 55–60 (1999).
35. L. Mosekilde, Sex differences in age-related loss of vertebral trabecular bone mass and structure—Biomechanical consequences. *Bone*. **10**, 425–432 (1989).
36. M. Ding, A. Odgaard, F. Linde, and I. Hvid, Age-related variations in the microstructure of human tibial cancellous bone. *J Orthop Res*. **20**, 615–621 (2002).
37. T. Kobayashi and H. Kronenberg, Minireview: Transcriptional regulation in development of bone. *Endocrinology*. **146**, 1012–1017 (2005).
38. T. Komori, H. Yagi, S. Nomura, A. Yamaguchi, K. Sasaki, K. Deguchi, Y. Shimizu, R. T. Bronson, Y. H. Gao, M. Inada, M. Sato, R. Okamoto, Y. Kitamura, S. Yoshiki, and T. Kishimoto, Targeted disruption of Cbfa1 results in a complete lack of bone formation owing to maturational arrest of osteoblasts. *Cell*. **89**, 755–764 (1997).
39. K. Nakashima, X. Zhou, G. Kunkel, Z. Zhang, J. M. Deng, R. R. Behringer, and B. de Crombrugghe, The novel zinc finger-containing transcription factor osterix is required for osteoblast differentiation and bone formation. *Cell*. 108, 17–29 (2002).
40. Y. Gong, R. B. Slee, N. Fukai, G. Rawadi, S. Roman-Roman, A. M. Reginato, H. Wang, T. Cundy, F. H. Glorieux, D. Lev, M. Zacharin, K. Oexle, J. Marcelino, W. Suwairi, S. Heeger, G. Sabatakos, S. Apte, W. N. Adkins, J. Allgrove, M. Arslan-Kirchner, J. A. Batch, P. Beighton, G. C. Black, R. G. Boles, L. M. Boon, C. Borrone, H. G. Brunner, G. F. Carle, B. Dallapiccola, A. De Paepe, B. Floege, M. L. Halfhide, B. Hall, R. C. Hennekam, T. Hirose, A. Jans, H. Juppner, C. A. Kim, K. Keppler-Noreuil, A. Kohlschuetter, D. LaCombe, M. Lambert, E. Lemyre, T. Letteboer, L. Peltonen, R. S. Ramesar, M. Romanengo, H. Somer, E. Steichen-Gersdorf, B. Steinmann, B. Sullivan, A. Superti-Furga, W. Swoboda, M. J. van den Boogaard, W. Van Hul, M. Vikkula, M. Votruba, B. Zabel, T. Garcia, R. Baron, B. R. Olsen, and M. L. Warman, LDL receptor-related protein 5 (LRP5) affects bone accrual and eye development. *Cell*. **107**, 513–523 (2001).
41. W. M. Cheung, L. Y. Jin, D. K. Smith, P. T. Cheung, E. Y. Kwan, L. Low, and A. W. Kung, A family with osteoporosis pseudoglioma syndrome due to compound heterozygosity of two novel mutations in the LRP5 gene. *Bone*. **39**, 470–476 (2006).
42. H. Hartikka, O. Makitie, M. Mannikko, A. S. Doria, A. Daneman, W. G. Cole, L. Ala-Kokko, and E. B. Sochett, Heterozygous mutations in the LDL receptor-related protein 5 (LRP5) gene are associated with primary osteoporosis in children. *J Bone Miner Res*. **20**, 783–789 (2005).
42a. M. Kato, M. S. Patel, R. Levasseur, I. Lobov, B. H. Chang, D. A. Glass, 2nd, C. Hartmann, L. Li, T. H. Hwang, C. F. Brayton, R. A. Lang, G. Karsently, L. Chan. Cbfa1-independent decrease in osteoblast proliferation, osteopenia, and persistent embryonic eye vascularization in mice deficient in Lrp5, a Wnt coreceptor. *J Cell Biol.* **157,** 303–314 (2002).
43. P. Babij, W. Zhao, C. Small, Y. Kharode, P. J. Yaworsky, M. L. Bouxsein, P. S. Reddy, P. V. Bodine, J. A. Robinson, B. Bhat, J. Marzolf, R. A. Moran, and F. Bex, High bone mass in mice expressing a mutant LRP5 gene. *J Bone Miner Res*. **18**, 960–974 (2003).
44. M. Tate, T. A. Adamson Jr, and T. W. Bauer, Cells in focus. The Osteocyte. *IJBCB*. **36**, 1–8 (2004).
45. T. A. Franz-Odendaal, B. K. Hall, and P. E. Witten, Buried alive: How osteoblasts become osteocytes. *Dev Dyn*. **235**, 176–190 (2006).
46. J. M. Quinn and M. T. Gillespie, Modulation of osteoclast formation. *Biochem Biophys Res Commun*. **328**, 739–745 (2005).
47. M. Zaidi, H. C. Blair, B. S. Moonga, E. Abe, and C. L. Huang, Osteoclastogenesis, bone resorption, and osteoclast-based therapeutics. *J Bone Miner Res*. **18**, 599–609 (2003).
48. T. Wada, T. Nakashima, N. Hiroshi, and J. M. Penninger, RANKL-RANK signaling in osteoclastogenesis and bone disease. *Trends Mol Med*. **12**, 17–25 (2006).
49. T. J. Martin and N. A. Sims, Osteoclast-derived activity in the coupling of bone formation to resorption. *Trends Mol Med*. **11**, 76–81 (2005).
50. J. Rubin, C. Rubin, and C. R. Jacobs, Molecular pathways mediating mechanical signaling in bone. *Gene*. **367**, 1–16 (2006).
51. J. M. Weber, S. R. Forsythe, C. A. Christianson, B. J. Frisch, B. J. Gigliotti, C. T. Jordan, L. A. Milner, M. L. Guzman, and L. M. Calvi, Parathyroid hormone stimulates expression of the Notch ligand Jagged1 in osteoblastic cells. *Bone*. **39**, 485–493 (2006).
52. G. J. Atkins, P. Kostakis, B. Pan, A. Farrugia, S. Gronthos, A. Evdokiou, K. Harrison, D. M. Findlay, and A. C. Zannettino, RANKL expression is related to the differentiation state of human osteoblasts. *J Bone Miner Res*. **18**, 1088–1098 (2003).
53. A. M. Parfitt, Bone remodeling. *Henry Ford Hosp Med J*. **36**, 143–144 (1988).
54. J. Kragstrup and F. Melsen, Three-dimensional morphology of trabecular bone osteons reconstructed from serial sections. *Metab Bone Dis Relat Res*. **5**, 127–130 (1983).
55. A. M. Parfitt, The cellular basis of bone remodeling: The quantum concept reexamined in light of recent advances in the cell biology of bone. *Calcif Tissue Int*. **36** (Suppl 1), S37–45 (1984).

56. A. M. Parfitt, D. S. Rao, J. Stanciu, A. R. Villanueva, M. Kleerekoper, and B. Frame, Irreversible bone loss in osteomalacia. Comparison of radial photon absorptiometry with iliac bone histomorphometry during treatment. *J Clin Invest*. **76**, 2403–2412 (1985).
57. T. A. Einhorn and R. J. Majeska, Neutral proteases in regenerating bone. *Clin Orthop Relat Res*. 286–297 (1991).
58. E. F. Eriksen, *et al*., Reconstruction of the resorptive site in iliac trabecular bone: A kinetic model for bone resorption in 20 normal individuals. *Metab Bone Dis Rel Res*. **5**, 235–242 (1984).
59. R. W. Smith, Jr. and R. R. Walker, Femoral expansion in aging women. Implications for osteoporosis and fractures. *Henry Ford Hosp Med J*. **28**, 168–170 (1980).
60. C. B. Ruff and W. C. Hayes, Subperiosteal expansion and cortical remodeling of the human femur and tibia with aging. *Science*. **217**, 945–948 (1982).
61. M. P. Akhter, U. T. Iwaniec, M. A. Covey, D. M. Cullen, D. B. Kimmel, and R. R. Recker, Genetic variations in bone density, histomorphometry, and strength in mice. *Calcif Tissue Int*. **67**, 337–344 (2000).
62. M. C. van der Meulen, K. J. Jepsen, and B. Mikic, Understanding bone strength: Size isn't everything. *Bone*. **29**, 101–104 (2001).
63. J. E. Wergedal, M. H. Sheng, C. L. Ackert-Bicknell, W. G. Beamer and D. J. Baylink, Genetic variation in femur extrinsic strength in 29 different inbred strains of mice is dependent on variations in femur cross-sectional geometry and bone density. *Bone*. **36**, 111–122 (2005).
64. J. M. Geer and S. P. Timoshenko, *Mechanics of Materials*. PWS Publishing Company, Boston, 1990.
65. M. E. Levenston, G. S. Beaupre, and M. C. van der Meulen, Improved method for analysis of whole bone torsion tests. *J Bone Miner Res*. **9**, 1459–1465 (1994).
66. D. T. Reilly and A. H. Burstein, The elastic and ultimate properties of compact bone tissue. *J Biomech*. **8**, 393–405 (1975).
67. E. F. Morgan, O. C. Yeh, W. C. Chang, and T. M. Keaveny, Non-linear behavior of trabecular bone at small strains. *J Biomech Eng*. **123**, 1–9 (2001).
68. A. Odgaard, J. Kabel, B. an Rietbergen, M. Dalstra, and R. Huiskes, Fabric and elastic principal directions of cancellous bone are closely related. *J Biomech*. **30**, 487–495 (1997).
69. G. Yang, J. Kabel, B. Van Rietbergen, A. Odgaard, R. Huiskes, and S. Cowin, The anisotropic Hooke's law for cancellous bone and wood. *J Elasticity*. **53**, 125–146 (1999).
70. H. H. Bayraktar, A. Gupta, R. Y. Kwon, P. Papadopoulos, and T. M. Keaveny, The modified super-ellipsoid yield criterion for human trabecular bone. *J Biomech Eng*. **126**, 677–684 (2004).
71. T. M. Keaveny, E. F. Wachtel, S. P. Zadesky, and Y. P. Arramon, Application of the Tsai-Wu quadratic multiaxial failure criterion to bovine trabecular bone. *J Biomech Eng*. **121**, 99–107 (1999).
72. P. K. Zysset, M. S. Ominsky, and S. A. Goldstein, A novel 3D microstructural model for trabecular bone: II. The relationship between fabric and the yield surface. *Comput Methods Biomech Biomed Engin*. **2**, 1–11 (1999).
73. E. F. Morgan, D. N. Yetkinler, B. R. Constantz, and R. H. Dauskardt, Mechanical properties of carbonated apatite bone mineral substitute: Strength, fracture and fatigue behaviour. *J Mater Sci Mater Med*. **8**, 559–570 (1997).
74. J. C. I. Catanese, J. D. B. Featherstone, and T. M. Keaveny, Characterization of the mechanical and ultrastructural properties of heat-treated cortical bone for use as a bone substitute. *J Biomed Mater Res*. **45**, 327–336 (1999).
75. G. C. Reilly and J. D. Currey, The development of microcracking and failure in bone depends on the loading mode to which it is adapted. *J Exp Biol*. **202**, 543–552 (1999).
76. G. C. Reilly, Observations of microdamage around osteocyte lacunae in bone. *J Biomech*. **33**, 1131–1134 (2000).
77. K. Piekarski, Fracture of bone. *J Appl Phys*. **41**, 215–223 (1970).
78. W. E. Caler and D. R. Carter, Bone creep-fatigue damage accumulation. *J Biomech*. **22**, 625–635 (1989).
79. S. Nagaraja, T. L. Couse, and R. E. Guldberg, Trabecular bone microdamage and microstructural stresses under uniaxial compression. *J Biomech*. **38**, 707–716 (2005).
80. E. F. Morgan, O. C. Yeh, and T. M. Keaveny, Damage in trabecular bone at small strains. *Eur J Morphol*. **42**, 13–21 (2005).
81. A. Ascenzi and E. Bonucci, The tensile properties of single osteons. *Anat Rec*. **158**, 375–386 (1967).
82. A. Ascenzi and E. Bonucci, The compressive properties of single osteons. *Anat Rec*. **161**, 377–391 (1968).
83. A. Ascenzi, A. Benvenuti, F. Mango, and R. Simili, Mechanical hysteresis loops from single osteons: Technical devices and preliminary results. *J Biomech*. **18**, 391–398 (1985).
84. A. Ascenzi, P. Baschieri, and A. Benvenuti, The torsional properties of single selected osteons. *J Biomech*. **27**, 875–884 (1994).
85. P. R. Townsend, R. M. Rose, and E. L. Radin, Buckling studies of single human trabeculae. *J Biomech*. **8**, 199–201 (1975).
86. K. Choi and S. A. Goldstein, A comparison of the fatigue behavior of human trabecular and cortical bone tissue. *J Biomech*. **25**, 1371–1381 (1992).
87. J. Y. Rho, R. B. Ashman, and C. H. Turner, Young's modulus of trabecular and cortical bone material: Ultrasonic and microtensile measurements. *J Biomech*. **26**, 111–119 (1993).
88. C. J. Hernandez, S. Y. Tang, B. M. Baumbach, P. B. Hwu, A. N. Sakkee, F. van der Ham, J. DeGroot, R. A. Bank, and T. M. Keaveny, Trabecular microfracture and the influence of pyridinium and non-enzymatic glycation-mediated collagen cross-links. *Bone*. **37**, 825–832 (2005).
89. A. Ascenzi and E. Bonucci, The shearing properties of single osteons. *Anat Rec*. **172**, 499–510 (1972).
90. X. N. Dong and X. E. Guo, Geometric determinants to cement line debonding and osteonal lamellae failure in osteon pushout tests. *J Biomech Eng*. **126**, 387–390 (2004).
91. J. L. Katz and A. Meunier, Scanning acoustic microscope studies of the elastic properties of osteons and osteon lamellae. *J Biomech Eng*. 115, 543–548 (1993).
92. P. K. Zysset, X. E. Guo, C. E. Hoffler, K. E. Moore, and S. A. Goldstein, Mechanical properties of human trabecular bone lamellae quantified by nanoindentation. *Technol Health Care*. **6**, 429–432 (1998).
93. J. Y. Rho, P. Zioupos, J. D. Currey, and G. M. Pharr, Variations in the individual thick lamellar properties within osteons by nanoindentation. *Bone*. **25**, 295–300 (1999).
94. C. H. Turner, J. Rho, Y. Takano, T. Y. Tsui, and G. M. Pharr, The elastic properties of trabecular and cortical bone tissues are similar: Results from two microscopic measurement techniques. *J Biomech*. **32**, 437–441 (1999).
95. S. Hengsberger, A. Kulik, and P. Zysset, Nanoindentation discriminates the elastic properties of individual human bone lamellae under dry and physiological conditions. *Bone*. **30**, 178–184 (2002).
96. Z. Fan, J. G. Swadener, J. Y. Rho, M. E. Roy, and G. M. Pharr, Anisotropic properties of human tibial cortical bone as measured by nanoindentation. *J Orthop Res*. **20**, 806–810 (2002).

97. B. Busa, L. M. Miller, C. T. Rubin, Y. X. Qin, and S. Judex, Rapid establishment of chemical and mechanical properties during lamellar bone formation. *Calcif Tissue Int*. **77**, 386–394 (2005).
98. J. Litniewski, Determination of the elasticity coefficient for a single trabecula of a cancellous bone: Scanning acoustic microscopy approach. *Ultrasound Med Biol*. **31**, 1361–1366 (2005).
99. T. Hofmann, F. Heyroth, H. Meinhard, W. Franzel, and K. Raum, Assessment of composition and anisotropic elastic properties of secondary osteon lamellae. *J Biomech*. **39,** 2282–2294 (2005).
100. G. Balooch, M. Balooch, R. K. Nalla, S. Schilling, E. H. Filvaroff, G. W. Marshall, S. J. Marshall, R. O. Ritchie, R. Derynck, and T. Alliston, TGF-beta regulates the mechanical properties and composition of bone matrix. *Proc Natl Acad Sci U S A*. **102**, 18813–18818 (2005).
101. T. Hoc, L. Henry, M. Verdier, D. Aubry, L. Sedel, and A. Meunier, Effect of microstructure on the mechanical properties of Haversian cortical bone. *Bone*. **38**, 466–474 (2006).
102. L. Weiss, *Cell and Tissue Biology, A Textbook of Histology*. Urban and Schwarzenberg, Baltimore, 1988.
103. E. F. Morgan, J. J. Lee, and T. M. Keaveny, Sensitivity of multiple damage parameters to compressive overload in cortical bone. *J Biomech Eng*. 127, 557–562 (2005).